A Finite Element Tool for Investigation of Vortex-Induced Vibration of Marine Risers

George Kwok-Chee Lee

THE NORWEGIAN UNIVERSITY
OF SCIENCE AND TECHNOLOGY
DEPARTMENT OF ENGINEERING DESIGN
AND MATERIALS

MASTER THESIS SPRING 2014
FOR
STUD.TECHN. GEORGE LEE

A FINITE ELEMENT TOOL FOR INVESTIGATION OF VORTEX INDUCED VIBRATION OF MARINE RISERS
Et elementmetodebasert verktøy for beregning av hvirvelinduserte vibrasjoner av stigerør

Vortex Induced Vibration (VIV) is a major design issue for all deep-water riser systems operating in regions where severe sea currents can be expected. Cross-flow vibrations occurring during lock-in of the vortex shedding frequency and natural frequency of the riser can diminish the riser fatigue life, dictate the riser arrangement, fabrication details, vessel layout, installation method, and thus have a significant cost impact at all stages of the field development.

The main objective of the master thesis is to continue the development and implementation of the VIV methodology established as part of the preceding student project. The master thesis will address the following:
- extended code validation
- code refactoring to improve efficiency
- include structural response and convergence tests
- fatigue calculations
- VIV suppression
- implementation of VIV GUI in Fedem Software.

The thesis will be a multidisciplinary project combining such fields as fluid dynamics, offshore engineering, finite element analysis, fatigue design, and software development. The ultimate goal is to establish a fully integrated and commercial accessible VIV tool in Fedem Software.
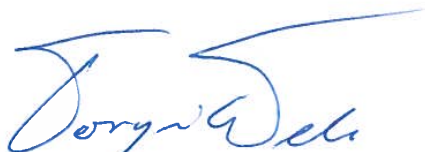
Three weeks after start of the thesis work, an A3 sheet illustrating the work is to be handed in. A template for this presentation is available on the IPM's web site under the menu "Masteroppgave" (http://www.ntnu.no/ipm/masteroppgave). This sheet should be updated one week before the Master's thesis is submitted.

Performing a risk assessment of the planned work is obligatory. Known main activities must be risk assessed before they start, and the form must be handed in within 3 weeks of receiving the problem text. The form must be signed by your supervisor. All projects are to be assessed, even theoretical and virtual. Risk assessment is a running activity, and must be carried out before starting any activity that might lead to injury to humans or damage to materials/equipment or the external environment. Copies of signed risk assessments should also be included as an appendix of the finished project report.

The thesis should include the signed problem text, and be written as a research report with summary both in English and Norwegian, conclusion, literature references, table of contents, etc. During preparation of the text, the candidate should make efforts to create a well arranged and well written report. To ease the evaluation of the thesis, it is important to cross-reference text, tables and figures. For evaluation of the work a thorough discussion of results is appreciated.

The thesis shall be submitted electronically via DAIM, NTNU's system for Digital Archiving and Submission of Master's thesis.

Contact person: Ken-Robert G. Jakobsen, Fedem Technology AS

Torgeir Welo
Head of Division

Bjørn Haugen
Supervisor

NTNU
Norges teknisk-
naturvitenskapelige universitet
Institutt for produktutvikling
og materialer

Preface

The present thesis is submitted to the Norwegian University of Science and Technology (NTNU), for the degree of Master of Science in Engineering and ICT, spring 2014. This work has been carried out at the Department of Engineering Design and Materials, in collaboration with Fedem Technology AS.

This is a continuation of the project work from autumn, 2013, and makes use of the simulation software FEDEM Software developed by Fedem.

Trondheim, June 10, 2014

George Lee

THE NORWEGIAN UNIVERSITY OF SCIENCE AND TECHNOLOGY

Abstract

Faculty of Engineering Science and Technology
Department of Engineering Design and Materials

M.Sc.

**A FINITE ELEMENT SOFTWARE TOOL FOR INVESTIGATION OF
VORTEX-INDUCED VIBRATION OF MARINE RISERS**

by George Lee

Vortex-induced vibration (VIV) is a major design issue for all deep-water riser systems operating in regions where severe sea currents can be expected. This highly complex phenomenon has resulted in a great deal of experimental work that today's empirical models are based upon. These models are based on frequency domain dynamic solutions and are therefore not directly applicable in a non-linear time domain model.

The purpose of the present work is to develop an approach to combine frequency domain models with a time domain analysis software in order to predict VIV, and implement this into a procedure named FEDEM-VIV. A force prediction algorithm is developed to compute VIV response amplitudes with the Newmark time integration algorithm in FEDEM Software.

A validation study is carried out to compare the results from FEDEM-VIV with VIVANA - a frequency domain code. Damping due to large amplitude is pragmatically handled. Response shapes are for this reason not well captured, but maximum response amplitudes are in some cases close to VIVANA estimates. High number of iterations will in general over-estimate the response, and high amplitude damping is not predicted well. Defining a lower limit of the excitation coefficient for damping, with a low iteration limit showed feasible predictions of the excitation force distribution. Excitation zone predictions in VIVANA and FEDEM-VIV are in good agreement.

With these simplifications in mind, the current approach represents a good solution for a time domain VIV predictor when all the essential hydrodynamical effects are accounted for in FEDEM-VIV.

NORGES TEKNISK-NATURVITENSKAPELIGE UNIVERSITET

Sammendrag

Fakultet for ingeniørvitenskap og teknologi

Institutt for produktutvikling og materialer

M.Sc.

Et elementmetodebasert verktøy for beregning av virvelinduserte vibrasjoner av stigerør

av George LEE

Virvelinduserte vibrasjoner (VIV) er en utfordring for dypvannsbaserte stigerør i havområder som er utsatt for sterke strømninger. Dette komplekse naturfenomenet har gitt opphav til flere eksperimenter som dagens empiriske modeller baserer seg på. Disse modellene er definert i frekvensdomenet til dynamiske løsninger og kan derfor ikke anvendes direkte i en ikke-lineær tidsdomene.

Hensikten med denne oppgaven er å utvikle en metode som kombinerer modeller fra frekvensdomenet med et analyseprogram som kjører i tidsdomenet. Dette skal implementeres som et programvareverktøy kalt FEDEM-VIV. En algoritme for å forutsi kraft er utviklet for å beregne responsamplitude ved hjelp av Newmarks tidsintegrasjonsalgoritme i FEDEM Software.

En valideringsstudie er utført for å sammenligne resultater fra FEDEM-VIV med VI-VANA - en frekvensdomenebasert kode. Dempninger som følge av store amplituder er håndtert på en pragmatisk måte. Svingningsformer er ikke godt estimert, men maksimal responsamplitude samsvarer i enkelte tilfeller godt med anslagene fra VIVANA. Generelt vil mange iterasjoner overvurdere svingningene, og dempning som følge av stor amplitude er ikke godt nok dekket. Ved å sette en nedre grense for eksitasjonskoeffisienten ved dempning med få iterasjoner, har dette gitt brukbare estimater av lastfordelingen for eksitasjon. Beregnede eksitasjonssoner i VIVANA og FEDEM-VIV samsvarer godt.

Med tanke på disse forenklingene er denne metoden en god løsning på et tidsdomenebasert verktøy for å beregne VIV, når alle essentielle hydrodynamiske effekter er inkludert.

Acknowledgements

I would like to thank Fedem Technology for making it possible to perform this thesis and especially my supervisor Ken-Robert G. Jakobsen from Fedem Technology, for excellent support, follow-up and encouragement. His knowledge of hydrodynamics has been of great value to me. The working space provided by Fedem is gratefully appreciated.

I would also like to thank Ole-Ivar Holthe, Knut Morten Okstad and Runar H. Refsnæs for their availability, support and valuable advice. Their nice working atmosphere is greatly appreciated, and this thesis would not have been possible without the insight and experience in FEA and FEDEM by Okstad.

At last, but not least, I would like to extend my gratitude to my supervisor at the department, Bjørn Haugen, for his ability to quickly understand the depth of a problem, help and guidance during this work.

Contents

List of Figures

List of Tables

Symbols

A	Area, cross-sectional
A	Amplitude
A_{CF}	Amplitude in cross-flow direction
A_y	Amplitude in y direction
(A/D)	Non-dimensional amplitude
$(A/D)_{C_L=0}$	Non-dimensional amplitude when $C_L = 0$
(A_y/D)	Non-dimensional amplitude in y direction
C_a	Added mass coefficient
C_D	Drag coefficient
C_{D0}	Local drag coefficient for fixed object
$C_{D,amp}$	Drag amplification coefficient
$C_{L,floor}$	Lift coefficient, lower limit
$\mathbf{C}$	System damping matrix
c_{hv}	Damping coefficient, high reduced velocity
c_{lv}	Damping coefficient, low reduced velocity
c_{sw}	Damping coefficient, still water
D	Diameter
D_o	Outer diameter of riser
D_i	Inner diameter of riser
E	Young's modulus
F	Force
F_D	Drag force per unit length
F^D	Damping force per unit length
F_L	Lift force per unit length
F_{tot}	Total excitation force per unit length
$\mathbf{F}^I$	Inertia forces matrix
$\mathbf{F}^D$	Damping forces matrix
$\mathbf{F}^S$	Elastic forces matrix
$\hat{f}$	Non-dimensional frequency

f_0, f_y	Natural frequency of cylinder
f_s, f_v	Vortex shedding frequency
f_{osc}	Oscillation frequency
G	Shear modulus
I_p	Polar moment of inertia
I_x	Second moment of area, with respect to x axis
I_y	Second moment of area, with respect y axis
k	Spring constant
K_s	Stability parameter
$\mathbf{K}$	System stiffness matrix
l, L	Length
$\mathbf{M}$	System mass matrix
m	Mass per unit length
m_a	Added mass per unit length
$\mathbf{Q}$	External forces matrix
r	Radius of cylinder
Re	Reynolds number
$\mathbf{r}$	Displacement matrix
S_t	Strouhal number
$S_{t,e}$	Strouhal number in Gopalkrishnan's tests
t	Time
T	Tension
U	Flow velocity
U_r	Reduced velocity
y	Displacement of cylinder in y direction
δ_r	Reduced damping
γ	Mode participation factor
γ_{exc}	Excitation parameter
ν	Kinematic viscosity
ν	Poisson's ratio
ω_s	Angular vortex shedding frequency
ω_y	Angular natural frequency
π	3.14159265...
ϕ	Phase angle
ρ	Density of water
ρ_{steel}	Density of steel
ζ	Structural damping factor

Chapter 1

Introduction

1.1 Background

As the search after oil and gas pushes offshore operators further out into deeper oceans, several challenges emerge. One of them is vortex-induced vibrations (VIV) of offshore structures such as marine risers due to ocean currents. A riser is a conduit that connects a production platform with the well at sea bed and is often subjected to large forces, due to currents and internal pressure. These vibrations are known to cause significant fatigue damage to structures that are exposed to waves and currents, in addition to increased drag load. Adjacent risers may also run the risk of colliding into each other with devastating consequences. The main effects of VIV are dictating riser arrangement, fabrication details, and thus have significant cost impacts at all stages. As water depth increases, the design and operation of risers gets more complex and VIV presents one of the biggest uncertainties facing riser engineers.

The methods for predicting VIV today are mostly based on empirical models from the early '80s. There is a long evolution from the simple two-dimensional cylinder section tests to today's models. However, as new riser configurations are developed to cope with increasing depths, more effort must be put into understanding the complex nature behind VIV as well as implementation and verification against experimental data.

1.2 Purpose

Fedem Technology AS desires a method to analyze VIV of risers in a more comprehensive way with their simulation software. The vision is to find an approach that could describe the essential effect behind VIV for practical engineering, and integrate such a model into

FEDEM Software to provide structural analyses as needed during design and verification of structures. The purpose of this thesis is therefore to develop and implement a method for predicting VIV of risers. With this, several domains of technology are relevant, such as hydrodynamics, finite element methods and software development. The thesis work is organized as follows:

1. Literature study on time and frequency domain analysis of VIV.

2. Code refactoring to improve efficiency.

3. Include structural response due to VIV.

4. Validation study.

Note that the scope of this thesis has been changed from the initial assignment text after consulting my supervisors. This is mainly due to the extensive work behind developing a VIV response analysis that must be validated through studies. A great effort has also been made into software development. Fatigue calculations and GUI implementations have been left out for this reason.

This report is therefore divided into an overview of the theoretical aspects of VIV, following a presentation of different analysis models and the implemented procedure in FEDEM Software, and ending with a validation study.

Chapter 2

Vortex-induced vibration

Vortex-induced vibration (VIV) is a phenomenon that occurs in many engineering situations that involves long flexible structures, such as cables, pipelines and risers. When structures are exposed to a subsonic flow, vortices are shed and create a vortex street behind the structure. The vortex shedding induces a motion to the structure, causing it to vibrate. For the offshore industry, VIV is a major design issue for all deep-water risers as they can potentially cause serious damage. A great deal of research work has been done in the last forty years to develop different methods to predict VIV and more is done to develop more accurate models.

2.1 Theoretical background

The classical case to illustrate VIV is a circular cylinder in constant current. As a fluid particle flows towards a cylinder, we can observe three major components. At the cylinder's leading edge, there is a zone of relative stagnation as the pressure of the upstream flow rises to stagnation pressure. The high pressure forces the fluid particle about the cylinder's lateral surfaces, in which the flow is laminar and smooth as boundary layers develop about both sides. Finally, just behind the cylinder lateral phase is the zone of separation, where turbulent vortices are generated as a laminar flow just upstream separates from the cylinder as parcel of fluids in rotational motion. The separation occurs in part because of the fluid behind the cylinder's trailing edge actually is moving in the opposite direction to the prevailing flow. When this retrograde flow encounters the prevailing flow, this imparts rotational motion to the fluid which separates as a vortex, known as a Kármán vortex street. These vortices interact with the cylinder, change the pressure distribution behind the cylinder and create lift and drag forces on the body.

Vortex shedding are for this reason the source of the phenomenon called vortex-induced vibration.

The vortex pattern generated by a cylinder with diameter D in a steady flow with velocity U is characterized by two parameters: the Reynolds number and the Strouhal number,

$$Re = \frac{UD}{\nu} \tag{2.1}$$

$$S_t = \frac{Df_s}{U} \tag{2.2}$$

where ν is the kinematic viscosity of the fluid and f_s is the vortex shedding frequency. The flow regimes are defined by the Reynolds number, which is illustrated in figure 2.1.

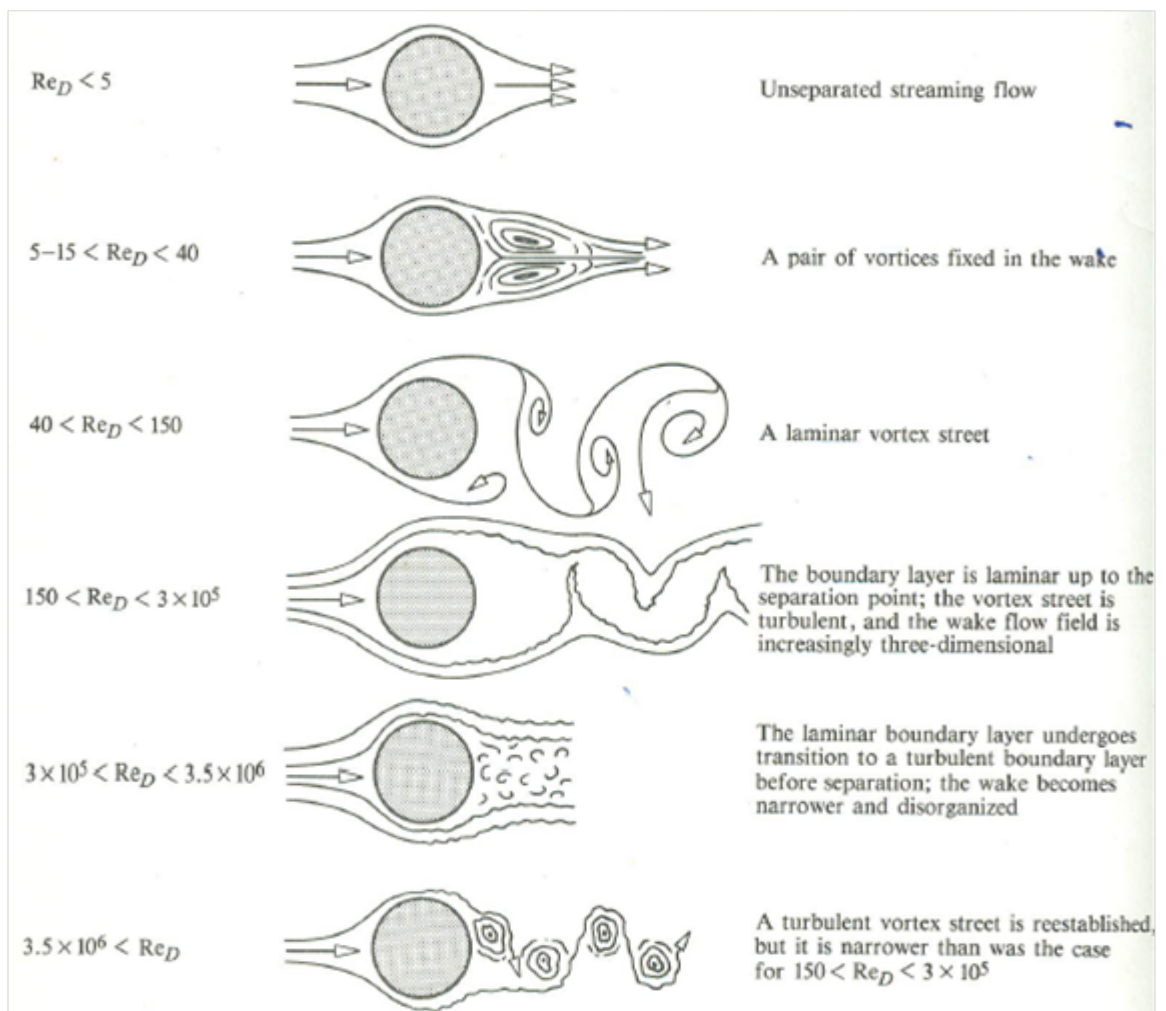| $Re_D < 5$ | | Unseparated streaming flow |
$5{-}15 < Re_D < 40$		A pair of vortices fixed in the wake
$40 < Re_D < 150$		A laminar vortex street
$150 < Re_D < 3 \times 10^5$		The boundary layer is laminar up to the separation point; the vortex street is turbulent, and the wake flow field is increasingly three-dimensional
$3 \times 10^5 < Re_D < 3.5 \times 10^6$		The laminar boundary layer undergoes transition to a turbulent boundary layer before separation; the wake becomes narrower and disorganized
$3.5 \times 10^6 < Re_D$		A turbulent vortex street is reestablished, but it is narrower than was the case for $150 < Re_D < 3 \times 10^5$

FIGURE 2.1: Regimes of fluid flow for different Reynolds number (Lienhard, 1966).

Most of the empirical models are derived from experimental work with Reynolds number in the sub-critical flow regime, that is for $300 < Re < 300000$. In real life however, conditions related to VIV are more likely to occur at higher flow regimes. Still, it is considered to be sufficient for our case of investigating riser VIV as experiments from a lower flow regime provide a more conservative approach. The Strouhal number is a dimensionless proportionality constant that is a function of Re. Even though this parameter to a lesser extent depends on the surface roughness of the cylinder, we can see that S_t is stable and close to 0.2 in the sub-critical flow regime. In addition, risers are designed with a sufficient roughness to provide a small increase of the vortex shedding frequency.
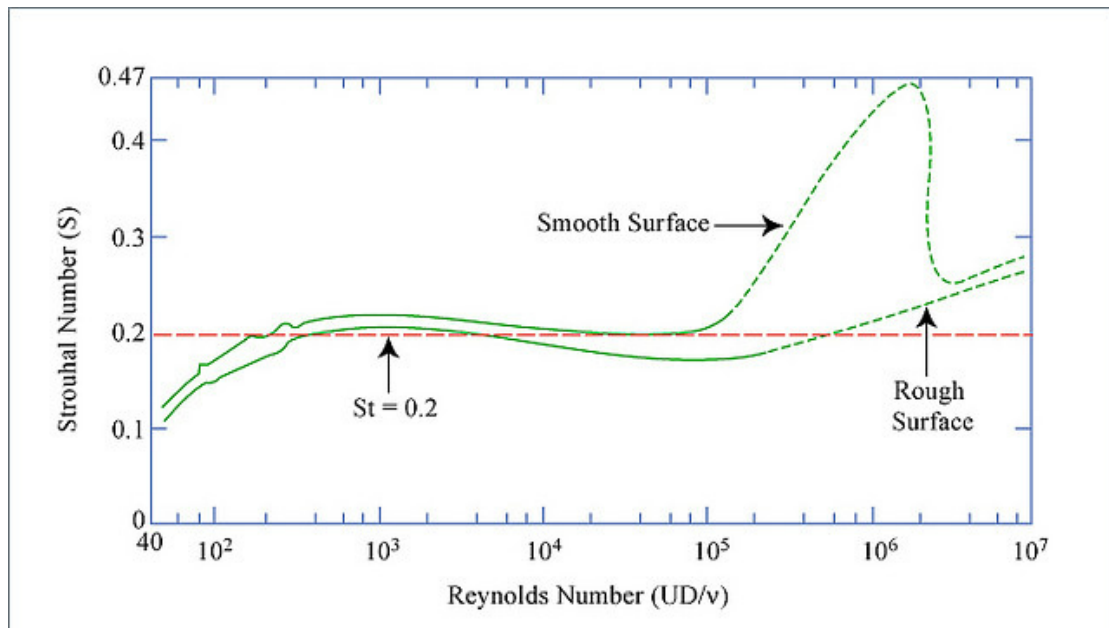
FIGURE 2.2: Strouhal number as a function of Reynolds number for circular cylinders (Lienhard, 1966; Achenbach and Heinecke, 1981).

2.1.1 Lock-in

When the shedding frequency f_s is close to an eigenfrequency f_0 of a cylinder, so that

$$f_0 \simeq f_s = \frac{S_t \cdot U}{D}, \tag{2.3}$$

resonance is caused on the cylinder so that it "locks in"[1]. The cylinder starts to oscillate with the same frequency as the shedding frequency, and can move both in-line and transverse to the flow direction. The latter is of greater concern as the cross-flow response has higher amplitude. With this in mind, VIV may be split into three types of motion:

- Cross-flow vibrations with vibration amplitude in the order of 1 diameter

- Pure in-line vibrations with amplitudes in the order of $10 - 15\%$ of the diameter

- Cross-flow induced in-line vibrations with amplitudes of $30 - 50\%$ of the cross-flow amplitude

Since the cylinder is moving, the shedding process is no longer related to the Strouhal number as opposed to a fixed cylinder case, but to the oscillation frequency. Hence, the shedding frequency is different from the fixed cylinder case. This is understood by the fact that the added mass in a free oscillating cylinder will vary such that the oscillation frequency will dictate the shedding process.

When a cylinder oscillates, the non-dimensional amplitude A/D is in general measured in the cross-flow direction. As the amplitude increases, at approximately one-half diameter and beyond, the symmetry of the vortex street begins to break up. This indicates that the vortex-induced forces on the cylinder is a function of the amplitude and furthermore, that the response caused by VIV is of a self-limiting type. If the amplitude is high enough, the fluid flow will no longer transfer energy to the cylinder but rather damps it.

2.1.2   Vortex-induced forces

The vortex-induced hydrodynamic forces on a cylinder can be decomposed into lift and drag forces. The lift force F_L per unit length is transverse to the oncoming flow direction and is given as

$$F_L = \frac{1}{2}\rho U^2 D C_L \tag{2.4}$$

where C_L is the lift coefficient. The lift force is considered to be in phase with the cross-flow velocity of the cylinder which means that if C_L is positive, F_L will add energy to the cylinder so it excites, while a negative coefficient will lead to damping. However, the ideal lock-in condition occurs when $C_L = 0$. No energy transmission between the cylinder and the fluid yields no lift or damping forces and we have a case that is similar to an undamped oscillator under steady state lock-in.

The drag force F_D per unit length is given as

$$F_D = \frac{1}{2}\rho U^2 D C_D \tag{2.5}$$

where C_D is the drag coefficient. Objects subjected to VIV will have a drag amplification $C_{D,amp}$ in addition to the local drag coefficient C_{D0} for a fixed object. That is

$$C_D = C_{D0} \cdot C_{D,amp} \tag{2.6}$$

Several empirical expressions for the drag amplification exist. The most common are described in [1]:

$$\text{Blevins (1990):} \qquad C_{D,amp} = 1 + 2.1 \left(\frac{A}{D} \right) \tag{2.7}$$

$$\text{Vandiver (1983):} \qquad C_{D,amp} = 1 + 1.043 \left(2 \frac{\sqrt{2}A}{D} \right)^{0.65} \tag{2.8}$$

2.1.3 Added mass

Submerged body that undergoes unsteady motion is experiencing inertia because it has to move some volume of the surrounding fluid as it moves through it. This effect is called added mass and is a function of the mass of the displaced fluid and the added mass coefficient C_a. In reality, the physical shape and mass of the submerged body remain unaffected as the added mass is merely an effect that describes the change of kinetic energy of the displaced fluid. For a cylinder, the added mass m_a per unit length is

$$m_a = \rho C_a \pi r^2 \tag{2.9}$$

where ρ is the fluid density and r is the radius of the cylinder. C_a is a function of the local flow velocity normal to the cylinder axis, the oscillation frequency and the cross section geometry. Depending on the direction of the flow of kinetic energy, C_a can be negative and is equal to unity for bodies under steady motion.

2.1.4 Fluid damping

When energy is dissipated during oscillation, the system is damped by three phenomena: fluid damping, internal material damping and structural damping. This subsection develops analysis for fluid damping due to vibrations in different flow regimes. Fluid damping is produced at the surface of the structure by viscous shearing of the fluid when vibrations in the fluid are damped. Venugopal proposed a semi-empirical model in 1996[2] as described in [3].

For still water damping, the coefficient is given as:

$$c_{sw} = \frac{\omega \rho \pi D^2}{2} \left[\frac{2\sqrt{2}}{\sqrt{Re_\omega}} + C_{sw} \left(\frac{A}{D} \right)^2 \right] \tag{2.10}$$

where the first part corresponds to the skin friction according to Stoke's law for drag forces and the second part is the pressure-dominated force. $Re_\omega = \omega D^2 / \nu$ where ω is the angular frequency of the cross-flow oscillation. Experiments have estimated the coefficient C_{sw} through curve fitting to be 0.25.

Damping coefficient in low reduced velocity regions is given by the still water case and a contribution from the incident flow velocity:

$$c_{lv} = c_{sw} + \rho D U C_{vl} \tag{2.11}$$

where measurements have shown the coefficient C_{vl} to be 0.18. Reduced velocity is defined as:

$$U_r = \frac{U}{D f_0} \tag{2.12}$$

Finally, damping coefficient in high reduced velocity regions is given as:

$$c_{hv} = \rho \frac{U^2}{\omega} C_{vh} \tag{2.13}$$

where measurements have shown the coefficient C_{vh} to be 0.2. Notice that this damping coefficient is independent of the non-dimensional amplitude.

For sufficiently large values of the amplitude ratio, the damping coefficient can be expressed with the lift coefficient by transforming the damping force $F^D = c_f \dot{y}$ into a equivalent lift force:

$$F_L = \frac{1}{2} \frac{\rho U^2 D C_L}{\omega A} \dot{y} \tag{2.14}$$

where $\dot{y}$ is the cross-flow damping velocity. $\frac{\dot{y}}{\omega A}$ is non-dimensional. By imposing the same energy loss per cycle, this implies that

$$c_f = -\frac{1}{2} \frac{\rho U^2 D C_L}{\omega A} \tag{2.15}$$

where C_L is negative.

2.1.5 Morison equation

The Morison equation is an empirical model for calculating in-line oscillatory wave forces on submerged bodies. For a moving body in oscillatory flow, the total in-line force per unit length is the sum of an inertia and drag force contribution, and the Froude-Krylov force respectively:

$$F(t) = m_a(\dot{u} - \dot{v}) + \frac{1}{2}\rho D C_D(u - v)|u - v| + \rho \pi r^2 \dot{u} \qquad (2.16)$$

where m_a is the added mass per unit length, $u(t)$ is the flow velocity and $v(t)$ is the velocity of the moving body with circular cross-section. Combining cross-flow forces with Morison forces describes the significant interaction between wave and structure.

2.2 Analysis of vortex-induced vibrations of risers

2.2.1 Equation of the free oscillating cylinder

The equation of motion for a rigid cylinder of single degree of freedom with linear springs and damping can be described as a sinusoidal process [4]:

$$m\ddot{y} + 2m\zeta\omega_y\dot{y} + k\,y = F_L\sin(\omega_s t) = \frac{1}{2}\rho U^2 D C_L\sin(\omega_s t), \qquad (2.17)$$

where

$$
\begin{aligned}
y &= \text{displacement of the cylinder in the vertical plane,} \\
m &= \text{mass per unit length of the cylinder, including added mass,} \\
\zeta &= \text{structural damping factor,} \\
k &= \text{spring constant,} \\
\omega_y &= 2\pi f_y = \text{angular natural frequency of cylinder,} \\
\omega_s &= 2\pi f_s = \text{angular shedding frequency,} \\
&\quad \text{and the overdots are notation for differentiation with respect to time.}
\end{aligned}
$$

The general solution to this equation can be found as a steady-state response with amplitude A_y and phase angle ϕ,

$$y = A_y\sin(\omega_s t + \phi) \qquad (2.18)$$

Inserting 2.18 into 2.17 yields (Thompson W. T., 1988)

$$\frac{y}{D} = \frac{\rho U^2 C_L \sin(\omega_s t + \phi)}{2k\sqrt{[1 - (\omega_s/\omega_y)^2]^2 + (2\zeta\omega_s/\omega_y)^2}} \tag{2.19}$$

where the phase angle can be expressed as

$$\tan\phi = \frac{2\zeta\omega_s\omega_y}{\omega_s^2 - \omega_y^2} \tag{2.20}$$

When the shedding frequency becomes nearly equal to the cylinders natural frequency, $f_s \approx f_y$, the response is at its maximum value and we get a state of resonance. Applying 2.18 with 2.19 and setting $f_y = (1/2\pi)\sqrt{k/m}$ gives an expression for the resonant vibration amplitude:

$$\left.\frac{A_y}{D}\right|_{f_y \approx f_s} = \frac{C_L}{4\pi S_t^2 \delta_r} \tag{2.21}$$

with reduced damping,

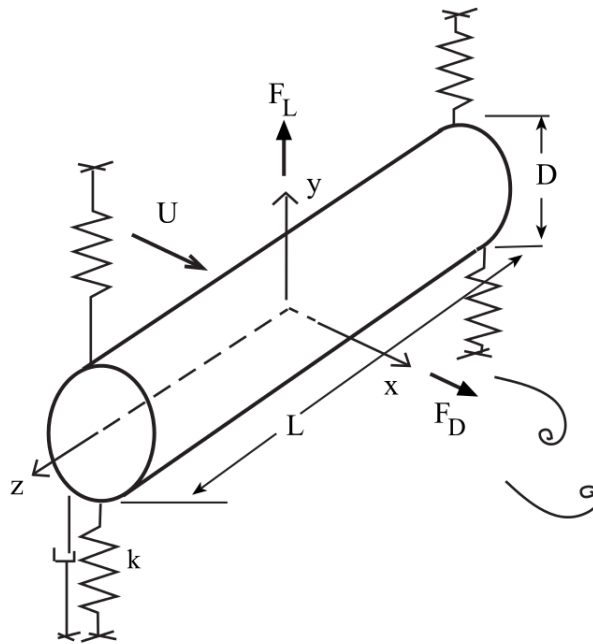$$\delta_r = \frac{2m(2\pi\zeta)}{\rho D^2} \tag{2.22}$$

FIGURE 2.3: Spring supported damped cylinder subjected to flow [5].

Notice also that the amplitude at resonance is independent of flow velocity. The reason is that fixing Strouhal number, to yield flow velocity U, also constrains the relationship between the shedding and the natural frequency of the cylinder.

We review the mechanisms behind resonance and when the shedding frequency and natural frequency lock on to each other. The cylinder's natural frequency will be influenced by the added mass as it varies for a given flow condition, and the oscillation itself will affect the shedding frequency. Therefore, the oscillation frequency is a natural frequency and also a shedding frequency valid for the actual flow condition during a state of resonance.

2.2.2 Forced oscillation

Obviously, there is a strong interaction between the lift force and amplitude. Several empirical methods for approximating the lift coefficient exist in addition to an iterative calculation model. What they share in common is that they do not come from free oscillation tests, but rather from forced motion experiments. Blevins derives in [1] a lift model based on several experimental response data from a cylinder. This model is developed by considering the energy input on a structure in motion to be the same. The lift curve can be determined by three coordinates, A, B and C, to plot two quadratic equations, intersecting at point B, so that a C_L can be obtained as a function of A_y/D

$$C_L = A + B\left(\frac{A_y}{D}\right) + C\left(\frac{A_y}{D}\right)^2 \tag{2.23}$$

The lift force increases as the vibration and amplitude increase from zero to a maximum value of around half a diameter before the cylinder begins to outrun the shedding vortices, which is the self-limiting effect mentioned earlier. The lift force diminishes as the amplitude increases to approximately 0.9 diameter and lift coefficient approaches zero. The response here is at its maximum. If the amplitude exceeds this point, the phase of the lift force will shift and the cylinder experiences damping.
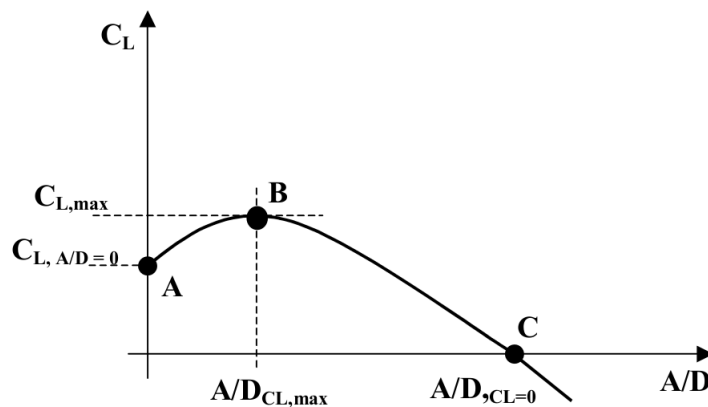

FIGURE 2.4: The lift coefficient model [6].

Blevins derived from experimental data from the '60s that the coefficients in the curve fit within a standard deviation of 0.07 to be

$$A = 0.35, \qquad B = 0.60, \qquad C = -0.93.$$

The interaction between different components of hydrodynamic forces, such as lift and drag, is governed by a balance between energy input and dissipation to provide dynamic equilibrium during VIV. This interaction is illustrated in figure 2.5 where there is an energy balance between excitation and damping zones of a structure.
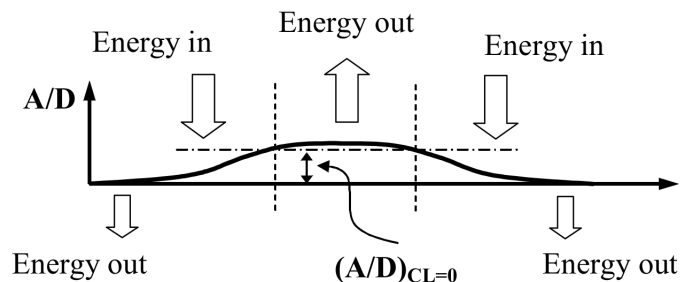

FIGURE 2.5: Energy balance for riser subjected to VIV in sheared current [7].

2.2.3 Decomposed lift forces

The total excitation force per unit length on a cylinder consists of two components that are in phase with, respectively, the oscillation velocity and acceleration. At each time step t, it is given as:

$$F_{tot}(t) = F_L \sin(\omega t) + m_a \omega^2 A_y \cos(\omega t) \tag{2.24}$$

2.3 Engineering practices

The purpose of this subsection is to present some applied methodologies for predicting VIV. A major role player of calculating risk in the maritime and energy industry is Det Norske Veritas (DNV GL). DNV GL describe itself as an *autonomous and independent foundation with the objectives of safeguarding life, property and the environment, at sea and onshore.* Since a large part of the industry adapt to rules and standards developed by DNV GL, it falls naturally to present some guidelines from it here.

DNV GL has developed several guidelines for analyzing VIV on marine risers. These publications cover *'proven technology and solutions which have been found by DNV GL to represent good practice'.* Recommended Practice DNV-RP-C205 'Environmental Conditions and Environmental Loads'[8] gives an extensive guidance for modeling, analysis

and prediction of environmental conditions. Rational design criteria and guidance for assessment of loads due to wind, wave and current on marine structures are also covered.

It also describes three computational models that can be used to predict VIV. The first is the *Response based models* where empirical models provide the steady state of VIV amplitude. Cross-flow and in-line vibrations are considered separately here. Secondly, is the *Force based models* where empirical data establish integrated force coefficients to obtain excitation, inertia and damping force values. It is recommended to use these models for strongly sheared flow, or flow where only parts of the structure are subjected to current. Lastly, is the *Flow based models* which are based on CFD.

The simple cross-flow VIV model in RP-C205 assumes that vortex shedding excitation may occur when $0.0625 \leq S_t \leq 0.333$, and the maximum response is normally found in the range $0.111 \leq S_t \leq 0.2$. The maximum response amplitude can be found as a function of the stability parameter K_s, which is also known as the damping factor δ_r mentioned earlier. See figure 2.6
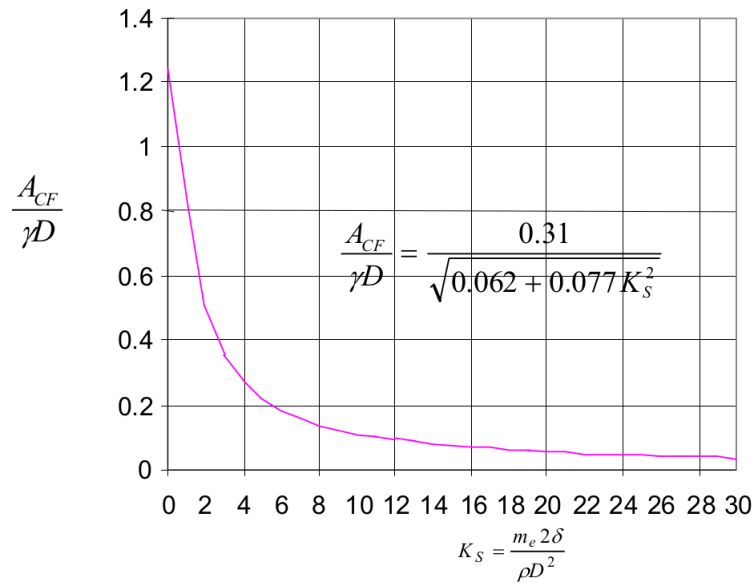
FIGURE 2.6: Amplitude as a function of K_s.

Furthermore, Offshore Standard DNV-OS-F201 'Dynamic Risers' suggest that the maximum response amplitude may be expressed as

$$\text{Sarpkaya (1979):} \qquad \frac{A_y}{D} = \frac{0.32\gamma}{\sqrt{0.06 + (2\pi S_t^2 \delta_r)^2}} \qquad (2.25)$$

where γ is the mode participation factor and is dependent on the geometry of the structure. Blevins lists in [1] different values of γ and is normally 1 for rigid cylinders.

A simple screening procedure for prediction of VIV can therefore be done by comparing the calculated eigenfrequencies of a riser with the shedding frequency, where $S_t \approx 0.2$. An approximation is that lock-in may occur if these frequencies matches a $\pm 20\%$ bandwith. If so, a closer investigation is needed. The main features of this procedure are somehow similar to the procedure described in Recommended Practice DNV-RP-F204 'Riser Fatigue'. There are however some special conditions that apply for the latter. That is, for top tensioned riser with constant diameter and it is particularly suitable for risers responding at mode no. 3 or higher.
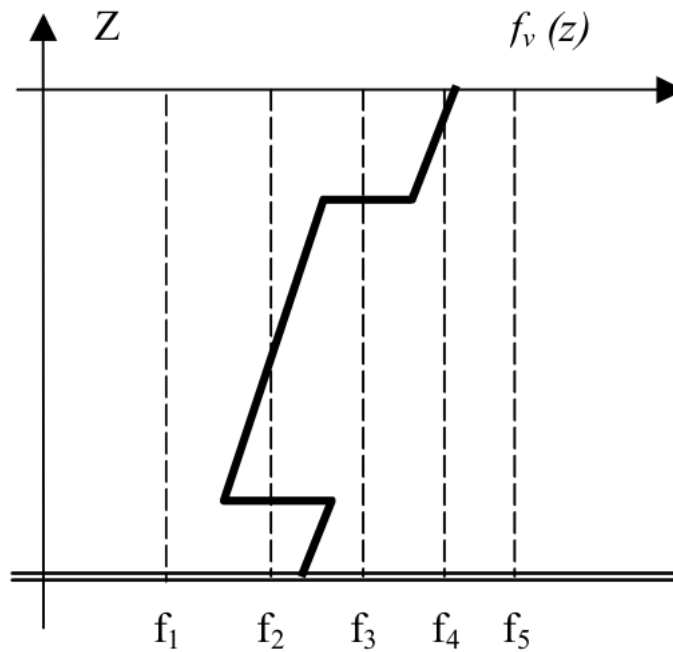

FIGURE 2.7: Map of vortex shedding frequency as a function of S_t, and eigenfrequencies $f_1, f_2, ..., f_5$.

With regards to drag, DNV GL recommends in DNV-RP-F203 'Riser Interference'[9] to apply Vandiver's expression, at equation no. 2.8, for calculating drag amplification.

Chapter 3

Utilizing FEM software to investigate riser VIV

The most common approach today for standard engineering tools to analyze VIV is to apply an empirical model for hydrodynamic forces with a FEM based structural model. Applying CFD to analyze VIV, especially for larger and more complex problem domain, are hardly seen as it would require a vast amount of computational resources. Figure 3.1 displays some of the available models within the frequency and time domain. Developed in 1999, ABAVIV remains as the only time domain program that is applied in practical engineering today in an area mostly dominated by frequency domain models [6]. This is because most of the empirical coefficients needed in a VIV analysis are available as functions of frequency. Applying these coefficients in a time domain model can for that reason not be done directly. Today, SHEAR7 describes itself as the offshore industry's leading software tool for the prediction of VIV [10].

Introduced in this chapter is an approach for investigating riser VIV based on the combination of applying hydrodynamical coefficients from modal analysis methods with a non-linear, time domain based, FEM software. The main aspects behind the VIVANA model[11] is presented as a basis for implementing the present VIV analysis procedure.
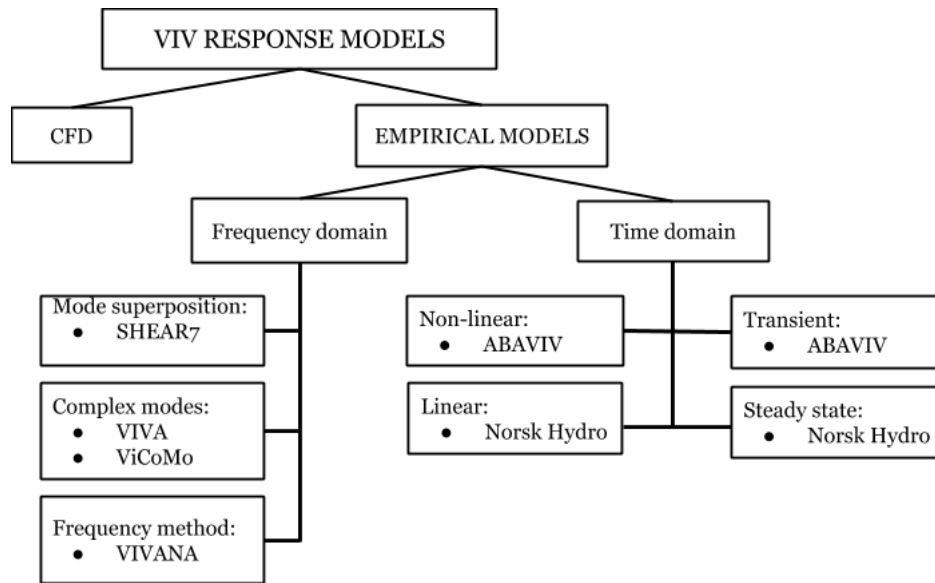
FIGURE 3.1: Overview of empirical VIV analysis programs[7].

3.1 FEDEM Software

FEDEM, an acronym for Finite Element Dynamics in Elastic Mechanisms, is a software for effective modeling, dynamic simulation and visualization of multi-body systems, i.e. finite element assemblies, and is developed by Fedem Technology. It utilizes a non-linear finite element formulation that predicts the dynamic response of elastic mechanisms experiencing non-linear effects.

Simulation of structures subjected to water and waves can be done in FEDEM Offshore^{TM}. Sea environment properties, such as wave and current functions, can be defined so that hydrodynamical loads on marine structures can be calculated. The Morison equation can be applied to produce inertia and drag forces on a structure. Risers can be modeled as a beam string consisting of multiple beam elements. Cross-sectional properties may be defined along with drag and added mass coefficients. In the following section, a brief explanation of how the dynamic simulation in FEDEM works is presented.

3.2 Non-linear time domain analysis

In FEDEM, step-by-step time integration methods are applied to solve non-linear problems in structural dynamics. An expression for the equation of motion on incremental form should be developed in order to use these numerical methods.

3.2.1 Dynamic equation on incremental form

The equation of dynamic equilibrium in a time domain, with time t, may be written as

$$\mathbf{F}^I(t, \mathbf{r}, \dot{\mathbf{r}}, \ddot{\mathbf{r}}) + \mathbf{F}^D(t, \mathbf{r}, \dot{\mathbf{r}}, \ddot{\mathbf{r}}) + \mathbf{F}^S(t, \mathbf{r}, \dot{\mathbf{r}}, \ddot{\mathbf{r}}) = \mathbf{Q}(t, \mathbf{r}, \dot{\mathbf{r}}, \ddot{\mathbf{r}}) \tag{3.1}$$

where

$$\begin{aligned}
\mathbf{F}^I &= \text{inertia forces,} \\
\mathbf{F}^D &= \text{damping forces,} \\
\mathbf{F}^S &= \text{elastic forces} \\
\mathbf{Q} &= \text{external loads and gravitational forces,} \\
\mathbf{r} &= \text{displacement,}
\end{aligned}$$

and the overdots are notation for differentiation with respect to time.

Equation (3.1) can be used to express the equilibrium at time $t_k(= kh)$, with a time step of length h, and t_{k+1} respectively. Subtracting them will produce the dynamic equation on incremental form:

$$\mathbf{\Delta F}_k^I + \mathbf{\Delta F}_k^D + \mathbf{\Delta F}_k^S = \mathbf{\Delta Q}_k \tag{3.2}$$

Expanding each term on the left-hand side of the equation yields the general form of the incremental (linearized) dynamic equation of motion

$$\mathbf{M}_k \Delta \ddot{\mathbf{r}}_k + \mathbf{C}_k \Delta \dot{\mathbf{r}}_k + \mathbf{K}_k \mathbf{\Delta r}_k = \mathbf{\Delta Q}_k \tag{3.3}$$

where $\mathbf{M}_k$, $\mathbf{C}_k$, $\mathbf{K}_k$ are the system mass, damping and stiffness matrix, respectively, at the beginning of time increment k, and $\mathbf{\Delta \ddot{r}}_k$, $\mathbf{\Delta \dot{r}}_k$ and $\mathbf{\Delta r}_k$ represents the change in displacement and its time derivative, during time increment k. By applying a time integration method to equation (3.3), we can solve $\mathbf{\Delta \ddot{r}}_k$, $\mathbf{\Delta \dot{r}}_k$ and $\mathbf{\Delta r}_k$. The total solution at the end of the increment is therefore:

$$\mathbf{r}_{k+1} = \mathbf{r}_k + \mathbf{\Delta r}_k \tag{3.4a}$$

$$\dot{\mathbf{r}}_{k+1} = \dot{\mathbf{r}}_k + \mathbf{\Delta \dot{r}}_k \tag{3.4b}$$

$$\ddot{\mathbf{r}}_{k+1} = \ddot{\mathbf{r}}_k + \mathbf{\Delta \ddot{r}}_k \tag{3.4c}$$

The forces at time $k + 1$ can be calculated from this solution. However, due to the linear approximation for the inertia, damping and stiffness relationship for each time increment, there are unbalanced forces at the end of the time increment. To correct this, the residual forces are added to the external load increment for the next step in

equation (3.3). Equation (3.3) can finally be expressed as

$$\mathbf{M}_k \Delta \ddot{\mathbf{r}}_k + \mathbf{C}_k \Delta \dot{\mathbf{r}}_k + \mathbf{K}_k \Delta \mathbf{r}_k = \mathbf{Q}_{k+1} - [\mathbf{F}_k^I + \mathbf{F}_k^D + \mathbf{F}_k^S] \tag{3.5}$$

3.2.2 Newmark integration algorithm

The Newmark β-family algorithm is applied in FEDEM to solve the dynamic equation from previous section by a step-by-step time integration scheme. The method applies Cauchy's mean value theorem to express the velocity and the displacement terms of said equation, such that the update scheme is as follows

$$\dot{\mathbf{r}}_{k+1} = \dot{\mathbf{r}}_k + (1 - \gamma)h\ddot{\mathbf{r}}_k + \gamma h\ddot{\mathbf{r}}_{k+1} \tag{3.6a}$$

$$\mathbf{r}_{k+1} = \mathbf{r}_k + h\dot{\mathbf{r}}_k + \left(\frac{1}{2} - \beta\right)h^2\ddot{\mathbf{r}}_k + \beta h^2\ddot{\mathbf{r}}_{k+1} \tag{3.6b}$$

where β and γ are integration parameters that are chosen for controlling stability, accuracy and efficiency for the integration. Newmark [12] showed that $\gamma = 0.5$ is a reasonable value and gives no artificial damping into the integration process. The same value is selected in the algorithm in FEDEM in addition to $\beta = 1/4$ which yields constant average acceleration and stability for linear systems.

3.3 VIVANA

VIVANA [11] is a response and FEM based model for calculation of VIV, fatigue damage and drag amplification of slender marine structures in current, and is developed by MARINTEK. Empirical coefficients are applied in the hydrodynamic model in VIVANA, while the structural model is based on a three-dimensional finite-element beam. The basic aspect and assumptions are:

- VIV is assumed to take place at discrete frequencies that are all eigenfrequencies, but with an added mass that is given by the local flow. The resulting response frequencies will therefore be an adjusted eigenfrequency.

- The current must be independent of time and act in the plane of the structure or perpendicular to this plane. The current may vary along the structure.

- Later versions of VIVANA have included both pure in-line and combined cross-flow and in-line VIV load in addition to the existing pure cross-flow load analysis.

- VIV response frequencies can occur concurrent or consecutive in a time sharing process.

- The main concept of energy balance as described earlier still applies, such that the structure can be divided into excitation and damping zones depending on the response frequency, local diameter and local flow velocity.

Before a brief outline of the VIVANA procedure is presented, an important parameter in VIVANA that should be introduced is the non-dimensional frequency. Empirical coefficients for the lift force, added mass and damping depend on this parameter. It is given as

$$\hat{f} = \frac{f_{osc}D}{U} \tag{3.7}$$

where f_{osc} is the oscillation frequency, D is the local diameter and U is the local flow velocity. The parameter can be seen as the inverse of reduced velocity. Since the coefficients for added mass and excitation force are found from experiments by Gopalkrishnan (1993) at a given Reynolds and Strouhal number, a correction of $\hat{f}$ must be done in order to use these data for other flow conditions. The non-dimensional frequency can be corrected for an actual Strouhal number, and expressed as:

$$\hat{f} = \frac{f_{osc}D}{U} \frac{S_{t,e}}{S_t} \tag{3.8}$$

where $S_{t,e}$ is the Strouhal number from the flow condition of the experiments that the coefficients are found from. In the newest version of VIVANA, $S_{t,e}$ is set to 0.2.

Added mass as a function of the non-dimensional frequency is established from forced motion tests of cylinder sections under an assumption that a constant amplitude of $A/D = 0.5$ is followed. The curve in figure 3.2 is used in VIVANA to account for added mass variation.
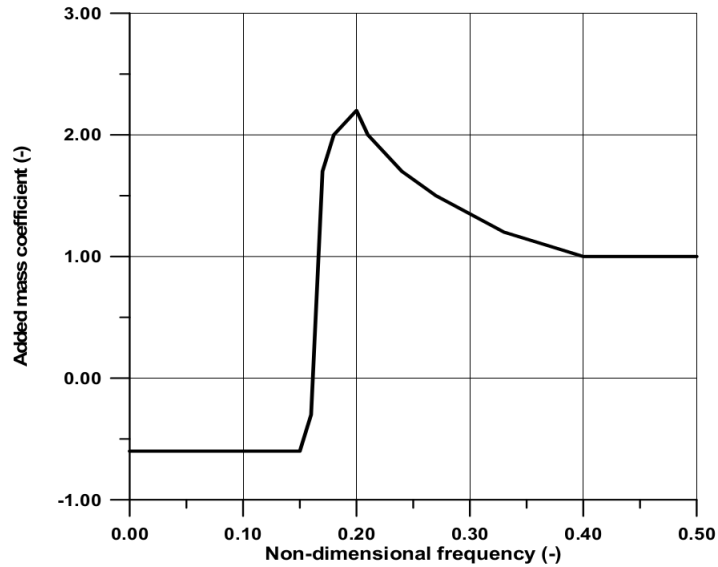
FIGURE 3.2: Added mass as a function of non-dimensional frequency (Gopalkrishnan)

The lift coefficient model in VIVANA is based on the same principle proposed by Blevins. The lift curve can be determined by three points, as a function of A/D. However, instead of applying the coefficients found by Blevins, the coefficients used in VIVANA are largely based on experimental works by Gopalkrishnan (1993) with some modifications by Vikestad (1998).

Recalling the lift coefficient model in figure 2.4, a lift curve can be constructed by applying the coefficients found by Gopalkrishnan and Vikestad, for a given non-dimensional response frequency. Figure 3.3 shows how these values can be found.
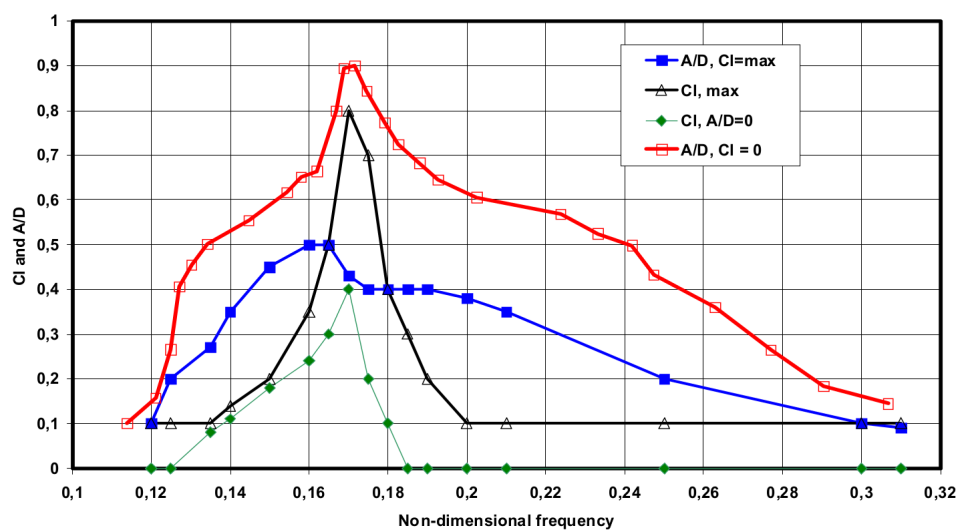

FIGURE 3.3: Definition of lift coefficients parameters.

Point A gives the lift coefficient value for zero response amplitude, i.e. the green curve, and point B is given by the response amplitude that gives maximum lift and the lift coefficient itself, i.e. the blue and black curve respectively. Finally, point C is given by the amplitude that gives zero lift, i.e. the red curve.

3.3.1 Method overview

A step-by-step procedure is given in the following.

Step 1. Static analysis A static equilibrium condition of the structure is performed by RIFLEX, an external analysis program.

Step 2. Eigenvalue analysis An eigenvalue analysis is done for the structure in still water.

Step 3. Identification of possible and dominating response frequencies Since added mass under VIV conditions is different from still water conditions, an iteration process is performed for each eigenfrequency found in step 2 to find new set of possible response frequencies. $\hat{f}$ is computed for each new frequency and chosen as a possible response frequency if it is within a user-defined range. In VIVANA 3.4, this is by default set to $[0.125 - 0.2]$, but newer versions, such as VIVANA 3.7, have extended this to $[0.125 - 0.31]$. The range selection is based on studies done by Gopalkrishnan (1993) where it can be shown that ideal lock-in occurs within a limited frequency bandwidth defined by $C_L = 0$. The dominating frequency is determined by the frequency that maximizes the excitation parameter γ_{exc}, defined as

$$\gamma_{exc} = \int_{L_E} U^3 D^2 \left(\frac{A}{D}\right)_{C_L=0} \mathrm{d}l \tag{3.9}$$

where $(A/D)_{C_L=0}$ is the amplitude that gives zero lift and can be found from figure 3.3, and L_E is the excitation length.

Step 4. Response calculation at the dominating frequency The frequency response method is used to calculate the dynamic response. Iteration is needed to solve the dynamic equilibrium equation and converges when the response is in accordance with the non-linear models for excitation and damping.

Step 5. Response calculation for other frequencies than the dominating Excitation may take place at other frequencies in zones outside the identified 'dominating' excitation zone. A similar calculation as for step 4 is done. Excitation zones already taken by more dominating frequencies are not recalculated.

Step 6. Fatigue analysis and post-processing Post-processing includes fatigue analysis and calculations of drag forces.

3.4 Procedure for VIV analysis: FEDEM-VIV

The procedure presented here, hereafter called FEDEM-VIV, is mainly based on the VIVANA model with the same lift coefficient parameters from figure 3.3. The response analysis is carried out in the time domain by the dynamics solver in FEDEM and a force prediction algorithm. Reuse of existing logic and routines in the FEDEM source code has been emphasized in order to avoid redundancy.

Algorithm 1 FEDEM Solver

Main driver for the FEDEM Dynamics Solver
1: Establish the initial configuration
2: **for each** time step **do** // Start of time integration loop
3:     Compute eigenvalues $\boldsymbol{\Omega}$
4:     **if** time = start time **then**
5:       Run FEDEM-VIV // Main driver for the VIV analysis
6:     **end if**
7:     Do one step of Newmark time integration
8: **end for**

The framework for the dynamic response analysis in FEDEM is shown in algorithm 1. It consists mainly of the time integration method as described earlier. Additional solver features, such as quasi-static analysis, is not described in this pseudocode.

FEDEM-VIV is implemented in Fortran 90 into FEDEM Software's source code as a module capable of analyzing FEDEM model files. The module is invoked during the first time step of the response analysis, as shown in line no. 5, when a set of eigenvalues are computed.

3.4.1 Space sharing between response frequencies

Since each response frequency will be associated to an excitation zone, it is necessary to determine which frequency that actually will become active when zones overlap. Results from model testing in [13] suggest that even though several response frequencies could become active, only one frequency, the dominating one, will be seen. This leads to

simultaneous active frequencies not having overlapping zones. The same principle is applied in FEDEM-VIV.

The set of response frequencies are sorted in increasing order of γ_{exc} values before a pruning process is applied to allocate frequencies to separate excitation zones. By looping through the set in such order, the frequency with smaller excitation parameter than the next frequencies in order will have its zone reduced if they are overlapping. The excitation zone of the dominating frequency will therefore not change.
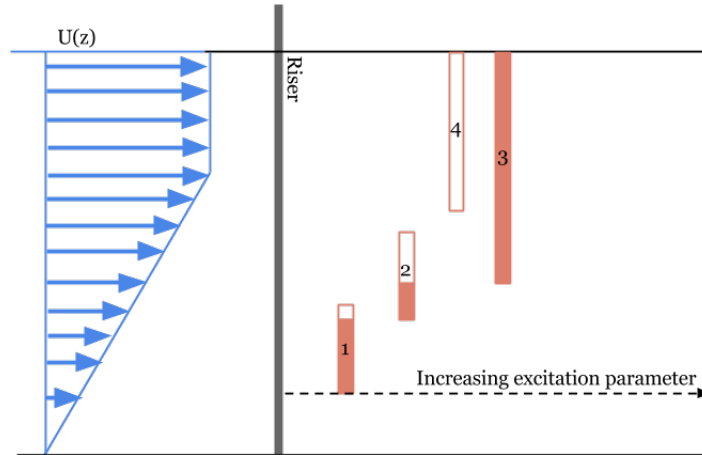

FIGURE 3.4: Excitation zones for space sharing frequencies

Figure 3.4 illustrates how the excitation zones for frequency 1, 2, 3 and 4 are allocated with this method. Frequency number 3 is the dominating response frequency and will keep its entire excitation length. Other frequencies will have their zones reduced.

3.4.2   Identifying the dominating response frequency

A pseudocode of the implemented procedure is shown in algorithm 2. It expects the eigenvalue analysis to calculate a set of eigenfrequencies to be given as input. Initially, the response frequency for each eigenmode is assumed to be the respective eigenfrequency. The corrected non-dimensional frequency for actual Strouhal number is calculated for each beam element along the riser, such that the added mass for each element is calculated and applied to the hydrodynamic mass matrix. When the total mass matrix of the riser is updated by calling the Morison forces routine, a new eigenvalue analysis is performed.

Algorithm 2 FEDEM-VIV - Compute dominating VIV response frequency

---

Input: Eigenfrequencies $\mathbf{\Omega}$.

Output: Dominating frequency ω_{Dom}.

1: $\hat{f}_{min} = 0.125$

2: $\hat{f}_{max} = 0.31$

3: $\omega_{Dom} = 0$

4: **for each** eigenfrequency $\omega \in \mathbf{\Omega}$ **do**

5:   **for each** beam element b **do**

6:     Assume that the response frequency is identical to ω:
   $$f_{osc} = \omega$$

7:     Compute non-dimensional frequency:
   $$\hat{f}(b) = \frac{f_{osc}D(b)}{U(b)}\frac{S_{t,e}}{S_t}$$

8:     Find added mass coefficient c_a as a function of $\hat{f}$

9:     Update beam inertia and damping forces $\Rightarrow \mathbf{F}^I, \mathbf{F}^D$

10:   **end for**

11:   Compute eigenvalues $\mathbf{\Omega}_a$

12:   **for each** eigenfrequency $\omega_a \in \mathbf{\Omega}_a$ **do**

13:     Accept ω_a as a possible response frequency:
   $$f_{osc} = \omega_a$$

14:     **for each** beam element b **do**

15:       $\hat{f}(b) = \frac{f_{osc}D(b)}{U(b)}\frac{S_{t,e}}{S_t}$

16:       **if** $\hat{f}_{min} \leq \hat{f}(b) \leq \hat{f}_{max}$ **then**

17:         Compute and increment excitation parameter:
   $$\gamma_{exc} = U^3 D^2 \left(\frac{A}{D}\right)_{C_L=0} \Delta L$$

18:       **end if**

19:     **end for**

20:   **end for**

21:   $\omega_{Dom} \Rightarrow max(\{\mathbf{\Omega}_a(\gamma_{exc})\})$

22:   Compute excitation zones for simultaneous acting frequencies.

23: **end for**

As seen, this process is done for each of the initially calculated eigenfrequencies, so that the procedure already runs in $\Theta(n^2)$ space. A new set of frequencies are calculated and the procedure recalculates the non-dimensional frequency to determine whether the new frequency is a possible response frequency. This is done in line no. 16. An energy criteria calculation is done to find the dominating response frequency. The dominating frequency is calculated from the non-dimensional frequencies that yields the largest value of γ_{exc}, see equation no. 3.9.

Once the dominating frequency has been identified, a dynamic response analysis is performed. In part 2 of the procedure, a lift coefficient curve is established for each non-dimensional frequency by solving three unknown points with three equations. Curve fitting is done for the imported data points in figure 3.3. The response amplitudes are calculated according to Sarpkaya. Finally, each beam element of the riser can be assigned a lift coefficient or a damping coefficient depending on the non-dimensional frequency.

3.4.3   VIV response analysis

VIVANA applies the frequency response method to perform dynamic response analysis. Nonetheless, it is a disadvantage that such methods cannot fully capture local non-linear behavior such as tension variation and endpoints interactions can cause [14]. In FEDEM however, the time domain analysis as implemented in the simulation software can take these nonlinearities into consideration. Excitation forces are applied as constant in time.
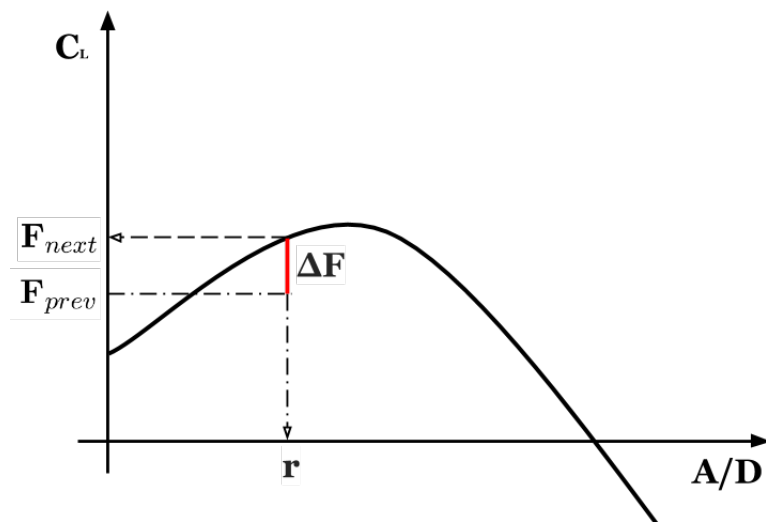

FIGURE 3.5: Update scheme of the force prediction algorithm

Recapturing the lift coefficient model of Blevins in chapter 2, where forced oscillation tests have given an empirical model for the lift force as a function of the amplitude. Based on this model, a force prediction algorithm is developed to predict the force needed to displace a body for a given amplitude. An illustration of the update scheme for the algorithm is shown in figure 3.5. An assumed initial force value F_{prev} is applied to a body to cause a displacement $\mathbf{r}$. The force is updated with the actual force value F_{next} for the measured displacement according to the lift coefficient curve. ΔF is the residual force that deviates from the actual lift function value. This iterative process is limited by the iteration step size as defined by the user. The algorithm then chooses the lift force that yields the smallest residual force value, and computes the resulting VIV response.

For sheared current profiles, a lift coefficient curve must be established for each discrete data of the current velocity. Hence, each node of a riser subjected to different current velocities must have its own lift curve. The residual force is now considered as an accumulation $\Sigma \Delta F$ of every nodal force prediction.

The force prediction algorithm is described in algorithm 3. The initial force vector $\mathbf{F}_{prev}$ is 0, which means that the force prediction iteration starts at point A from figure 2.4. For every force prediction iteration, the Newmark time integration routine is called to perform the response analysis. When a new lift coefficient is found for the resulting displacement $\mathbf{r}$, depending whether we have large amplitude damping or not, a new force value is computed and the residual force is incremented. Large amplitude damping occurs when C_L is negative such that $A/D > (A/D)_{CL=0}$ (cf. point C in figure 2.4) . The force vector with the lowest accumulated residual force is kept as $\sigma \Delta F$ and is the best prediction for an excitation force distribution.

The running time of the algorithm is asymptotically dependent on the number of time steps n in the Newmark time integration algorithm. On average, the algorithm runs in linear time $\mathcal{O}(n)$ for each iteration limit i.

Algorithm 3 FEDEM-VIV Force Prediction - Compute VIV response for ω_{Dom}

Input: Dominating frequency ω_{Dom} and its excitation parameters.

Output: Cross-flow response amplitude and lift coefficient distribution.

1: **for each** node n $\in$ excitation zone **do**

2:     Initialize equations of lift coefficient curve.

3:     Initialize new force component $\mathbf{Q}(n)$

4: **end for**

5: $\mathbf{F}_{prev} = 0$

6: $\Sigma \Delta F = 0$

7: **for** $i = 1$ to $nIterations$ **do**

8:     $t = t_{start}$

9:     **for each** node n $\in$ excitation zone **do**

10:        Set value to force component:
$$\mathbf{Q}(n) = \mathbf{F}_{prev}(n)$$

11:    **end for**

12:    Update external forces $\Rightarrow \mathbf{Q}$

13:    **while** $t < t_{end}$ **do**

14:        Do one step of Newmark time integration

15:        Update maximum response amplitude $\Rightarrow \mathbf{r}$

16:        Increment t

17:    **end while**

18:    **for each** node n $\in$ excitation zone **do**

19:        Find C_L as a function of $\mathbf{r}$

20:        **if** $C_L > 0$ **then**

21:            Compute excitation force:
$$\mathbf{F}_{next}(n) = \tfrac{1}{2}\rho U^2 D C_L \Delta L$$

22:        **else**

23:            Compute damping force:
$$\mathbf{F}_{next}(n) = \tfrac{1}{2}\frac{\rho U^2 D C_L \Delta L}{\omega_{Dom}\mathbf{r}}\dot{y}$$

24:        **end if**

25:        Increment $\Sigma \Delta F$:
$$\Sigma \Delta F = \Sigma \Delta F + abs(\mathbf{F}_{prev}(n) - \mathbf{F}_{next}(n))$$

26:    **end for**

27:    **if** $i = 1$ or $\Sigma \Delta F < \sigma \Delta F$ **then**

28:        Update $\sigma \Delta F = \Sigma \Delta F$

29:    **end if**

30:    $\mathbf{F}_{prev} = \mathbf{F}_{next}$

31: **end for**

Chapter 4

Verification study

4.1 Benchmark case

The benchmark case is reused from the initial project work[15] with some modification to the properties of the riser. The scenario is an oil field located northwest of Hammerfest in the Barents Sea with a mean water depth of 352 meters. A top tensioned riser (TTR), with no strakes, is subjected to a sheared current profile, called 2/3 current distribution because the first 1/3 of the water column has a constant velocity of 0.5 m/s, where the the remaining 2/3 of the water depth is linearly sheared to 0 m/s at sea floor. The verification study will analyze the TTR applied with two different tensions: (1) T = 440 kN and (2) T = 510 kN.
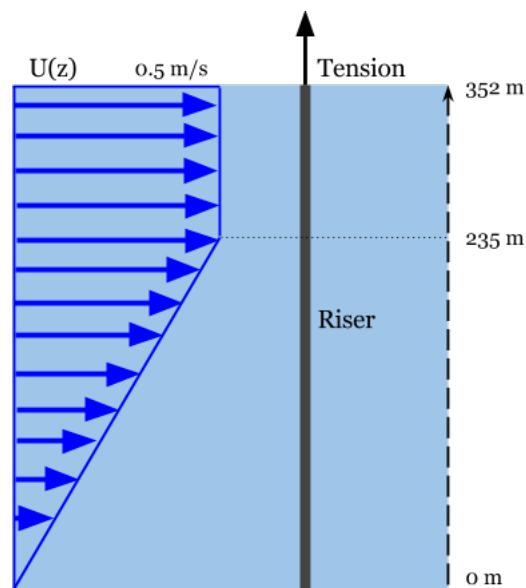

FIGURE 4.1: System overview of benchmark model

4.2 FEDEM model

In FEDEM, the system is simply modeled as a beam string with 176 beam elements subjected to the 2/3 current distribution. The total length of the riser is 352 meters. The bottom of the riser, at the wellhead, is fully fixed in all six degrees of freedom, and the top is constrained for translations in the horizontal plane and rotations in all directions. Hence, the top of the riser can only move vertically along z axis.
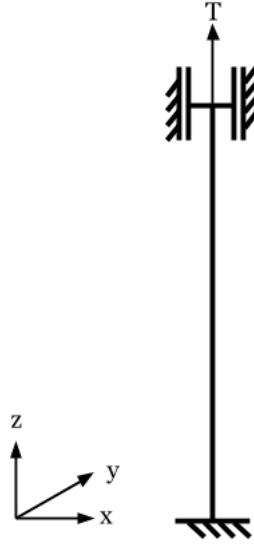

FIGURE 4.2: Riser model sketch and associated boundary conditions

The material property of the riser is given as

$$\rho_{steel} = 7\ 850\ \text{Kg/m}^3$$
$$\text{E} = 210\ \text{GPa}$$
$$\nu = 0.3125$$
$$\text{G} = 80\ \text{GPa}$$

where ρ_{steel} is the density of the casing material. In this case, there are no fluid, such as mud, in the riser.

The cross-section properties are

$$
\begin{aligned}
D_o &= 0.533 \text{ m} \\
D_i &= 0.495 \text{ m} \\
A &= 0.03068079 \text{ m}^2 \\
I_x &= 0.00101460 \text{ m}^4 \\
I_y &= 0.00101460 \text{ m}^4 \\
I_p &= 0.00202920 \text{ m}^4
\end{aligned}
$$

A tension force $T = 440$ kN is applied to the riser top, resulting in a tension force of roughly 400kN at the wellhead, according to [16]. The corresponding wellhead force is approximately 470 kN for $T = 510$ kN. The frequency bandwidth is set to $[0.125 - 0.31]$ and a total of 10 natural modes are calculated. The finished model in FEDEM can be seen in figure 4.3.
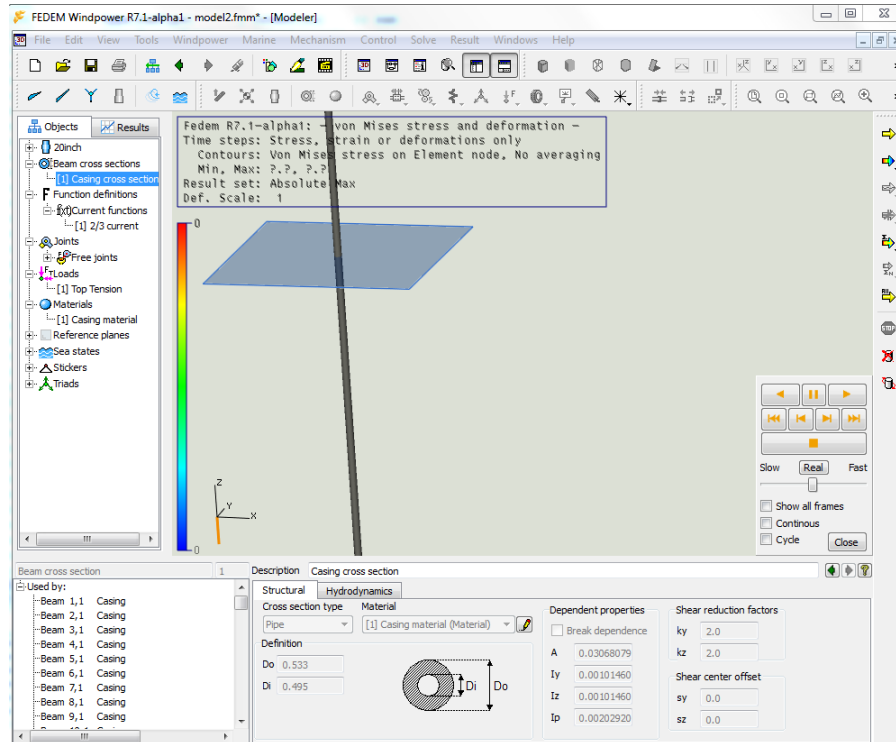

FIGURE 4.3: Riser modeled as beam elements in FEDEM

4.3 RIFLEX and VIVANA model

The input files to RIFLEX and VIVANA are configured to represent the same model as in FEDEM, with 176 elements and identical material properties. The same linear

axial force due to tension is applied in addition to rest of the boundary conditions. The hydrodynamical parameters are default data as given by VIVANA[11]. The kinematic viscosity is interpolated by VIVANA to be $1.56 \cdot 10^{-6} m^2/s$. All other parameters have default settings, such as relative structural damping being 1% and frequency response iteration is done with the fixed-point method.

4.4 Results: T = 440 kN

In the following will present the results from the analysis and a validation will be done. The main findings of the response frequency analysis are presented in the first subsection followed by the results of a thorough dynamic response analysis.

4.4.1 Response frequency results

The initial eigenvalue analysis for the TTR in still water gives the following natural frequencies in which added mass is applied to yield a new set of response frequencies. The computed excitation zones under the assumption that the response frequencies act concurrently are given in figure 4.5. It shows that each response frequency is allocated at different parts of the riser. VIVANA excitation zones are illustrated on the upper side of the axis, facing FEDEM-VIV zones below. Excitation zones for frequency number 1 and 2 corresponds well with each other, while FEDEM-VIV slightly underestimates the length of the fourth zone. Table 4.1 displays the result of the eigenvalue computation and γ_{exc} is the excitation parameter for each response frequency. We can observe that the dominating frequency appears to be 0.2627 Hz as it has the largest value of γ_{exc}.

VIVANA: T = 440 kN				
Freq. no.	Natural freq. [Hz]	Response freq. [Hz]	γ_{exc}	Length [m]
1	0.0693	0.0756	0.1373	56
2	0.1462	0.1484	0.5269	38
3	0.2368	0.2200	3.1021	16
4	0.3450	0.2627	3.9333	184
5	0.4730	0.3069	3.4738	0

TABLE 4.1: T = 440 kN, response data as computed by VIVANA

From table 4.1, we notice that frequency no. 5 has not been allocated an excitation zone. This is because the excitation zone of the dominating frequency overlaps completely no.

5's zone. Other frequencies have also had their lengths partly reduced as a consequence of the dominating frequency.

A set of 10 natural frequencies are computed, which resulted in 100 potential response frequencies as each natural frequency yields another 10 frequencies. Table 4.2 presents the results from the FEDEM-VIV analysis. The comparison between the natural frequencies from VIVANA and FEDEM-VIV are in good agreement, suggesting that the boundary conditions for both TTR models to be the same. However, the response frequencies computed here are slightly different from VIVANA, especially for frequency no. 4. VIVANA estimated this frequency to be 0.2627 Hz in contrary to 0.3109 Hz in FEDEM-VIV. Several factors might affect why the response frequency from these two disagree, but a verification in FEDEM-VIV should be limited to how the system mass matrix is defined. Damping forces should be neglected in an eigenvalue analysis and the elastic forces (stiffness matrix) should be unchanged. Since FEDEM-VIV applies the same added mass coefficient database as VIVANA, the difference in response frequencies can be found by investigating the subroutine in FEDEM that updates the Morison forces in line 9 of algorithm 2. The resulting excitation lengths will also be an effect of the differences we see for the response frequencies.

FEDEM-VIV: T = 440 kN				
Freq. no.	Natural freq. [Hz]	Response freq. [Hz]	γ_{exc}	Length [m]
1	0.0693	0.0811	0.1585	50
2	0.1462	0.1496	0.5418	38
3	0.2368	0.2141	2.9610	32
4	0.3449	0.3109	3.3991	171
5	0.4728	0.3270	3.1201	0

TABLE 4.2: T = 440 kN, response data as computed by FEDEM-VIV

Figure 4.4 illustrates the setup for the TTR under the assumption that the dominating response frequency $f_{osc} = 0.2627$ Hz. The corrected non-dimensional frequency $\hat{f}$ is shown and defines the excitation and damping zone for the system. The transition from excitation to damping occurs at 168 m. The lower part of the TTR, where $\hat{f} > \hat{f}_{max}$, experiences low reduced velocity damping.

	Response freq. [Hz]	Length [m]
VIVANA	0.2627	184
FEDEM-VIV	0.3109	171

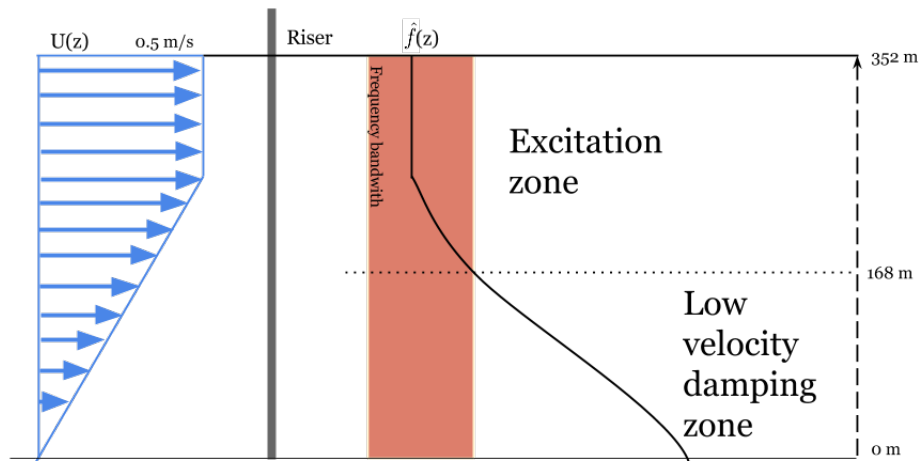TABLE 4.3: T = 440 kN, comparison of dominating VIV response

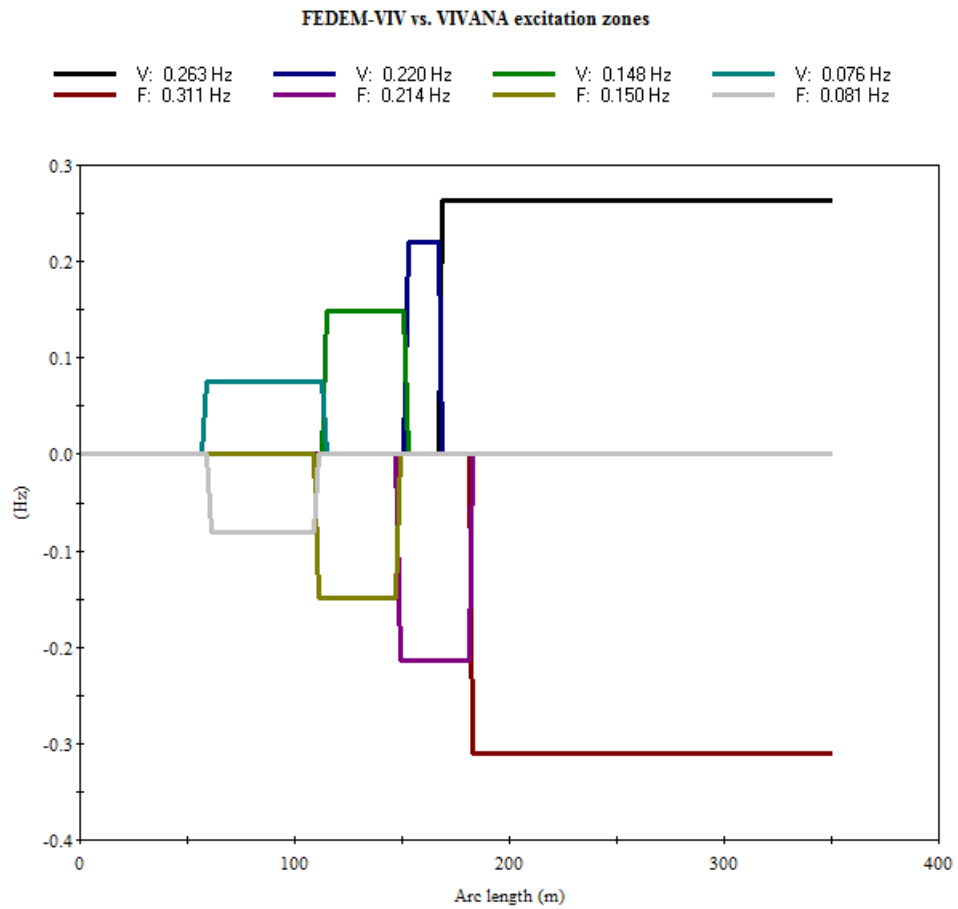FIGURE 4.4: Damping and excitation zone for riser with $f_{osc} = 0.2627$ Hz

FIGURE 4.5: Comparison of excitation zones, T = 440 kN

For verification purposes, the rest of the VIV analysis of T = 440 kN TTR in FEDEM-VIV will apply the results from VIVANA such that viable comparisons can be made. The dominating response frequency to be further investigated is henceforth $f_{osc} = 0.2627$ Hz with an excitation length of 184 m. The distribution of added mass coefficients along the TTR is identical on both analysis and is given in figure 4.6.
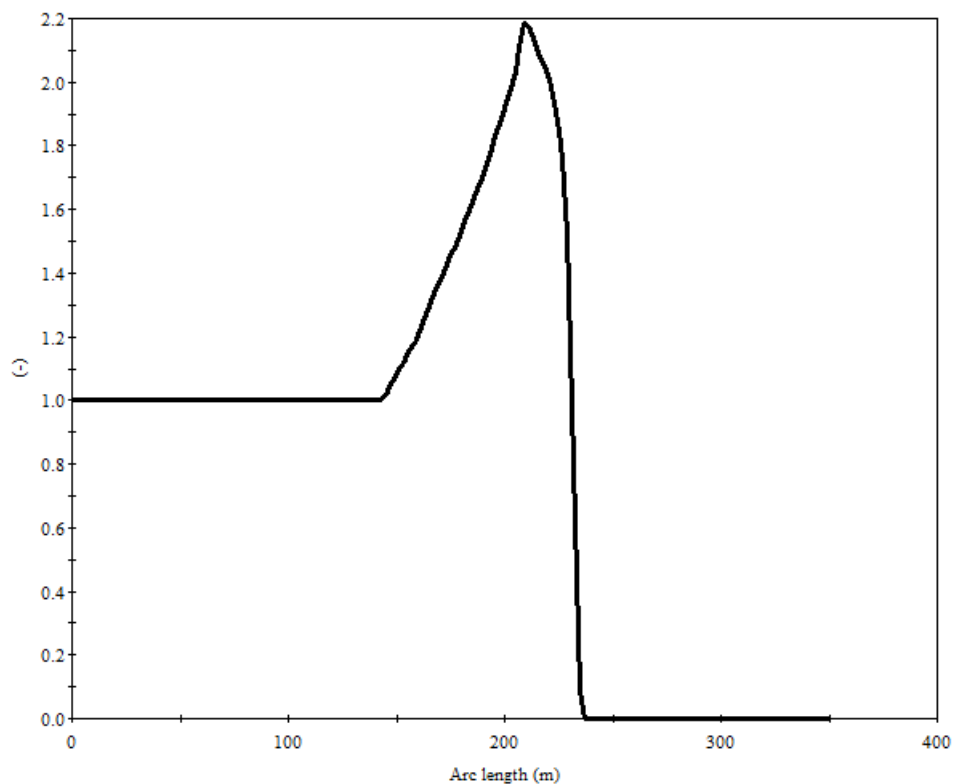
FIGURE 4.6: Added mass coefficient for response frequency 0.2627 Hz, T = 440 kN

4.4.2 Dynamic response results

As part of the verification study, a set of test cases for FEDEM-VIV is developed to see how many iterations of the force prediction algorithm is necessary to yield a converged force distribution. Large amplitude damping in excitation areas is differentiated by defining two set of criteria: (1) where $C_L = -0.05$ for any $A/D > (A/D)_{CL=0}$, such that the damping force is constant, and (2) where we introduce a lower limit of the excitation coefficient, $C_{L,floor} = -0.1$. For $C_L > C_{L,floor}$, the actual value is applied to calculate the damping. This pragmatic approach can be explained by the self-limiting response of VIV. Carlsen explains in [7] that the response amplitude of circular cylinders in general will not exceed $A/D = 1.2$. In addition, SHEAR7 version 4.4 has implemented $C_{L,floor} = -0.1$ as default setting. Table 4.4 gives an overview of the test cases.

Case	Iteration limit	Criteria for $C_L < 0$
1	64	fixed: $C_L = -0.05$
2	200	fixed: $C_L = -0.05$
3	256	fixed: $C_L = -0.05$
4	64	$C_{L,floor} = -0.1$
5	200	$C_{L,floor} = -0.1$

TABLE 4.4: T = 440 kN, FEDEM-VIV test cases

Each test simulation is set to run for 4 seconds with a time step of 0.1 seconds. 4 seconds is assumed to be sufficiently long enough for the system to reach steady-state vibration for the given response frequency. Figure 4.7 illustrates the oscillation shapes for each time series as computed by VIVANA, confirming that maximum amplitude can be observed after 3.81 seconds. A longer simulation length will also ensure potential initial instability effects of the system to disappear, as the excitation forces are constant and applied instantly to the system.
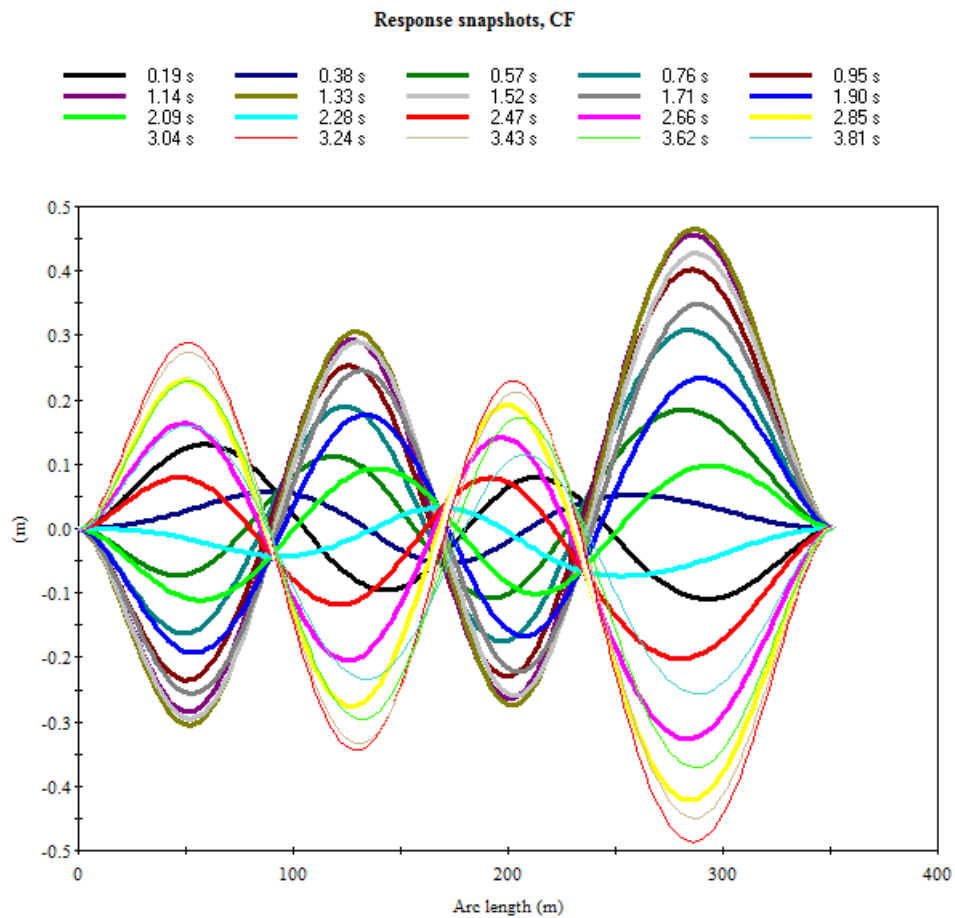
FIGURE 4.7: Snapshot for different time step, T = 440 kN

Results from case 1, and a comparison of case 2 and case 3 are presented in figure 4.8 and 4.9. In case 1, the minimal residual force distribution is found after 30 iterations.

However, further increments can improve the prediction as the dynamic response after 30 iterations, shown in figure 4.8, suggests a rather undervalued response compared to oncoming VIVANA results. The force distribution for a fixed C_L seems to converge after 166 iterations as figure 4.9 shows close to same response shape as after 227 iterations.
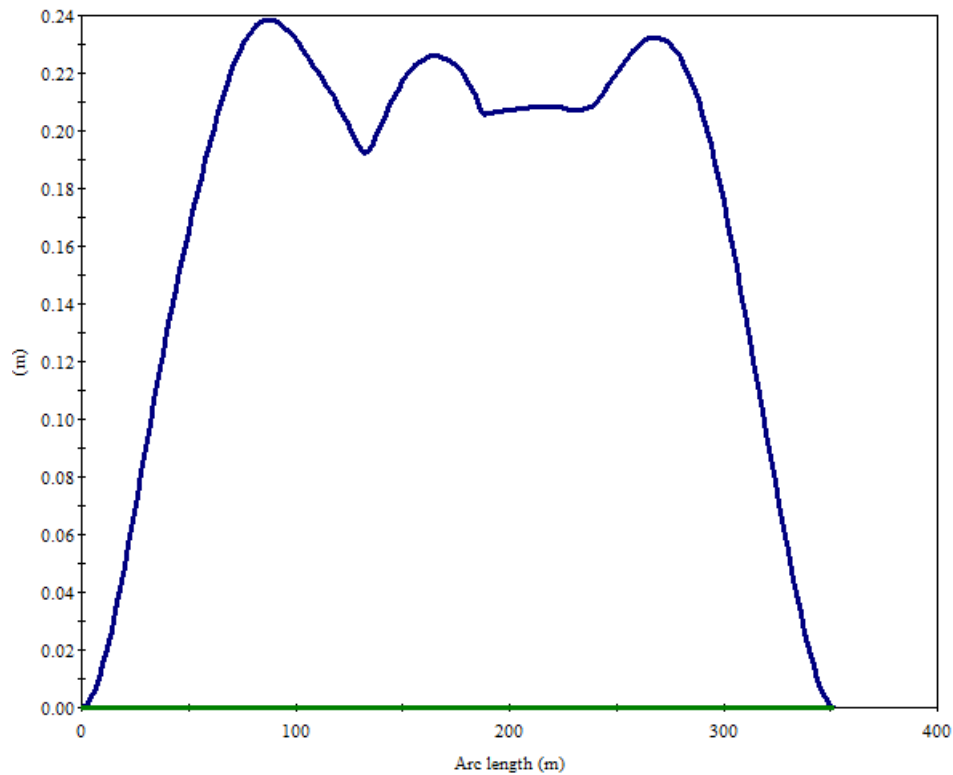

FIGURE 4.8: Case 1 - Max. nodal displacements after 30 iterations, T = 440 kN

A comparison of the response shape between FEDEM-VIV and VIVANA is shown in figure 4.10. The location of the large peaks on the TTR are somehow offset, but have slightly the same maximum values as computed in VIVANA. The response frequency corresponds to mode 4, in which four local extreme points are observed in the VIVANA response shape, as opposed to the three local peaks found in FEDEM-VIV. This may be explained by the constant excitation force in FEDEM-VIV that lacks periodic variation and phase shift, whereas these effects are accounted for in VIVANA through the frequency response method. The excitation force in FEDEM-VIV is applied as constant in terms of time and direction as a pragmatic way to measure maximum amplitude in a time domain. A deviation of approximately 8% is found for the local maximal amplitudes between these two analysis. Absolute maximum amplitude according to VIVANA is 0.47 m, or $A/D = 0.88$.

Figure 4.11 and 4.12 show the excitation force distribution for each iteration limit in case 1, and case 2 compared with case 3. As mentioned, the converged force distribution
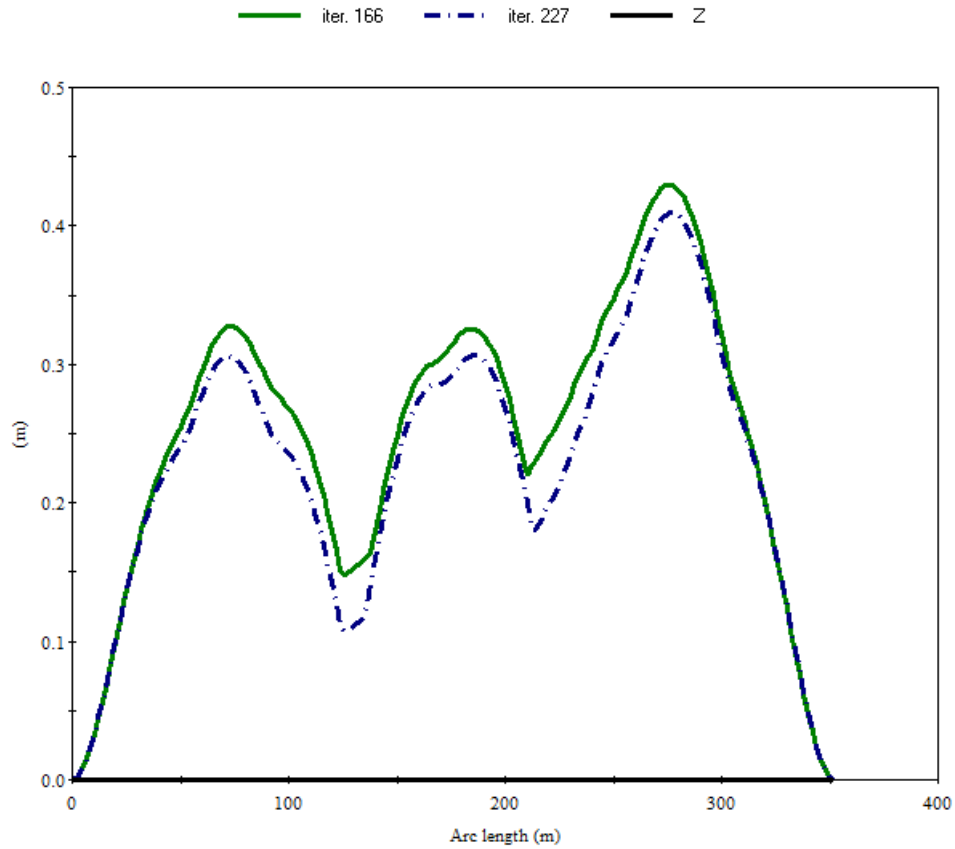
FIGURE 4.9: Case 2 and case 3 - Comparison of max. nodal displacements, T = 440 kN

can be seen after 166 iterations. Negative value of the lift force implies damping and acts in the opposite direction.

Setting a fixed $C_L = -0.05$ for all values of $C_L < 0$ has an effect of reducing the total energy added to the system, since the contribution from damping is significantly smaller. The excitation force distribution after 166 and 227 iterations can therefore be considered as an underestimation of what it would be in reality since the force needed to oscillate a riser is smaller in order to obtain dynamic equilibrium.

Moving onto the next lift force criteria, the resulting force distribution with $C_{L,floor} = -0.1$ from case 4 and 5 are illustrated in figure 4.14 and 4.16. After 19 iterations in case 4, the excitation force distribution agrees better with the result from VIVANA than the previous force distributions with fixed C_L. A comparison between the force distribution from case 4 and VIVANA is shown in figure 4.14. VIVANA seems not to differentiate between lift and damping forces in the graphical presentation, but FEDEM-VIV indicates that large amplitude damping is seen between 168 and 188 meter mark of the riser. This is consistent with the response shape at the same area. From the same figure, a maximum peak can be found acting at the same beam element of the TTR
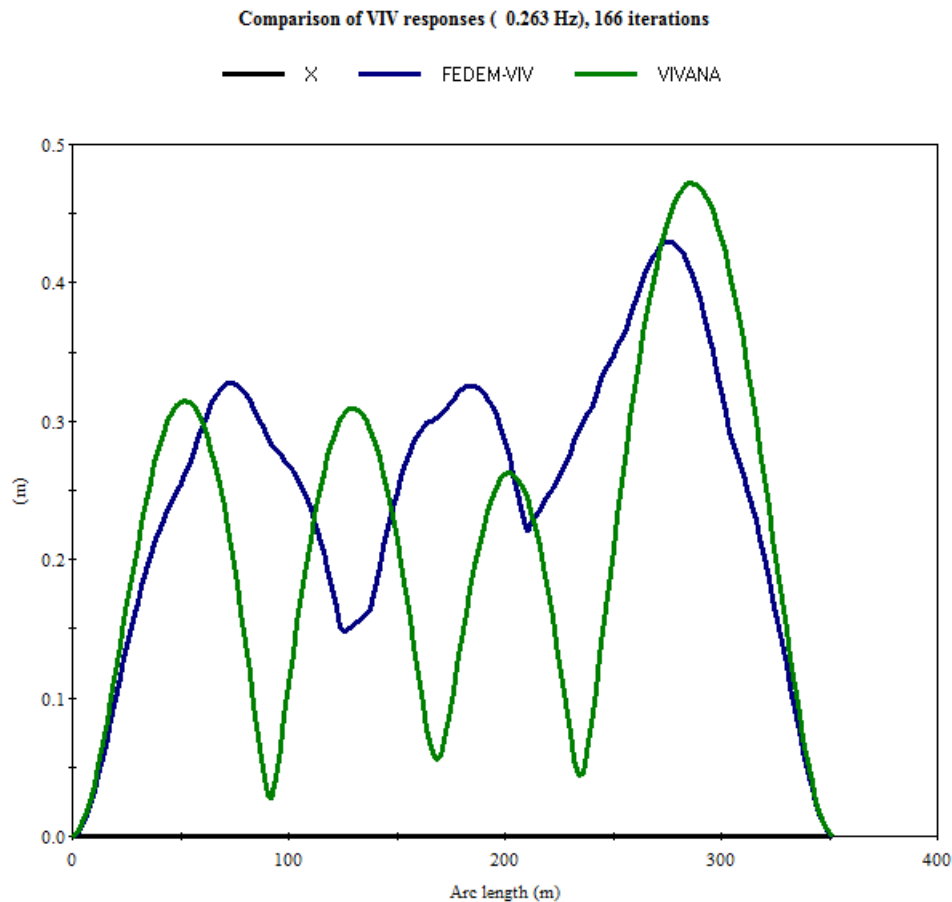
FIGURE 4.10: Comparison of responses for frequency 0.2627 Hz, T = 440 kN

as in VIVANA, and the same nodal forces can be seen close to sea level. The resulting maximum amplitude of 0.45 m, or $A/D = 0.84$ can be seen in figure 4.13. Again, the response shape in case 4 is not well captured, but the location of maximum amplitude seems to be close to VIVANA.

Results from case 5 are shown in figure 4.15 and 4.16 and is a rather unlikely response with $A/D > 2$. However, this case is included in the results as it shows the effect of high number iterations where damping forces are contributing in a larger scale than for the fixed coefficient case. Further work into controlling negative lift coefficients as a parameter is necessary. This is reflected by SHEAR7 setting the negative lift coefficient as a user-defined parameter. FEDEM-VIV suggests in case 5 damping and lift forces exceeding 100 N per beam element length, a rather conservative estimation.
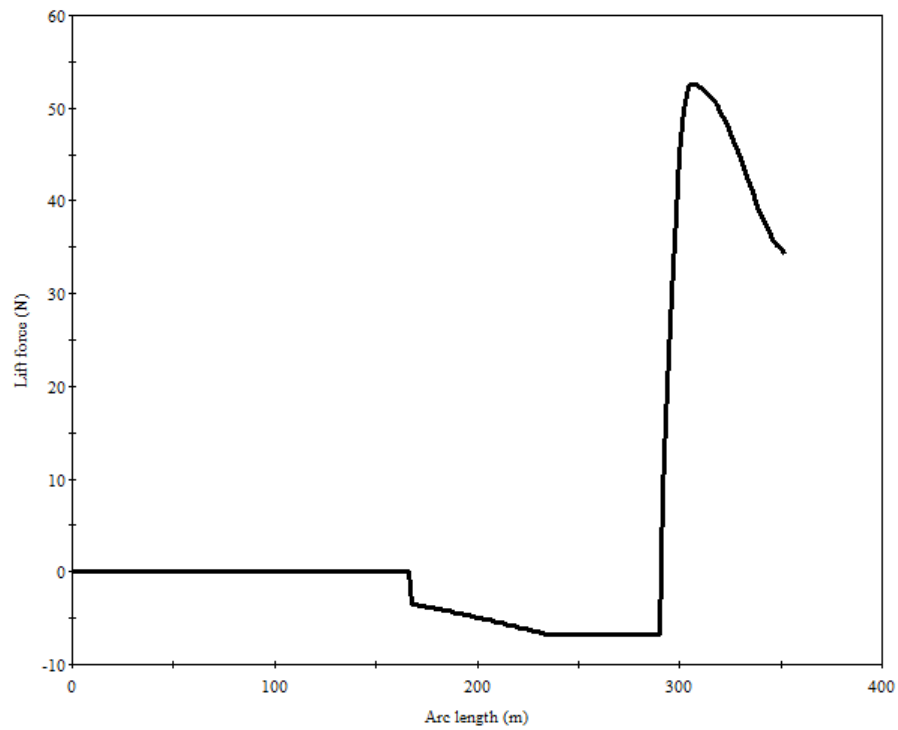
FIGURE 4.11: Case 1 - Excitation force distribution after 30 iterations, T = 440 kN
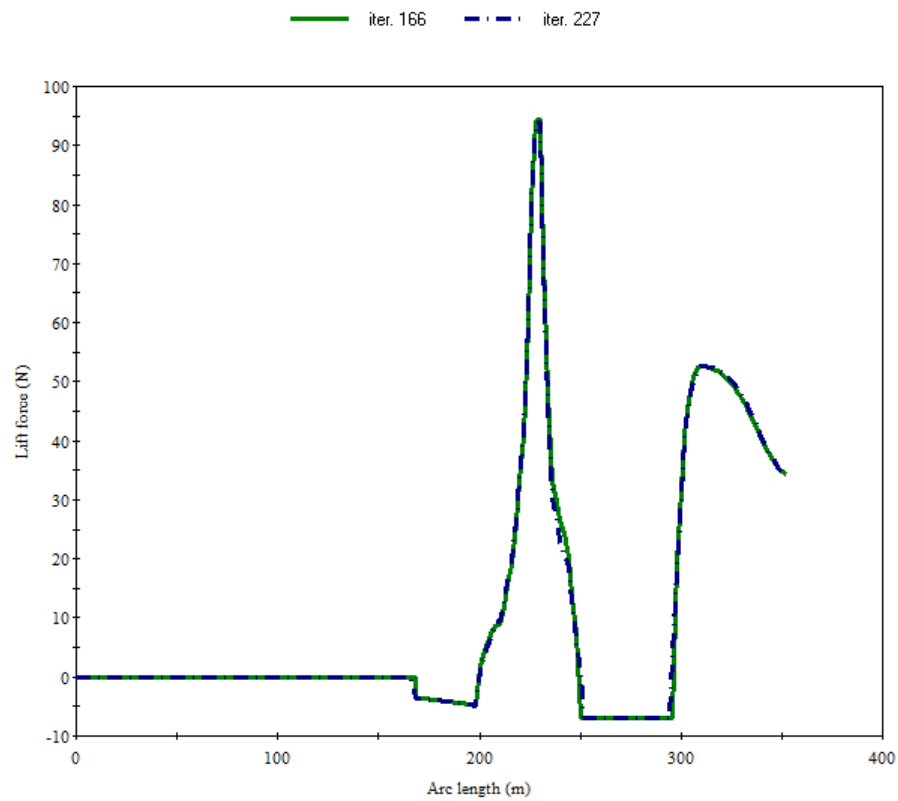
FIGURE 4.12: Case 2 and case 3 - Comparison of excitation force distributions, T = 440 kN
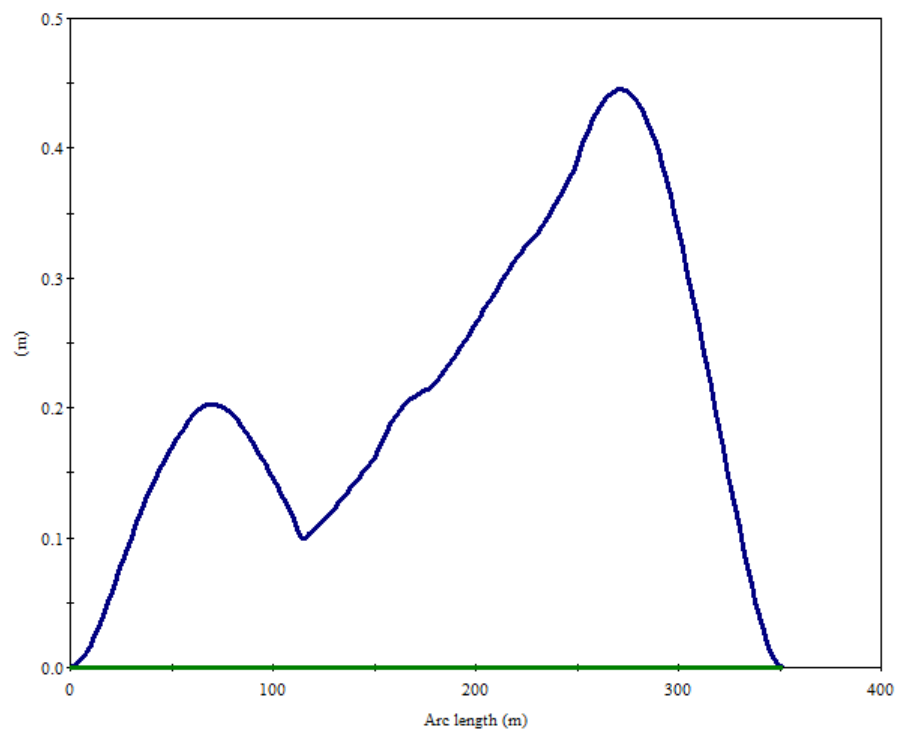
FIGURE 4.13: Case 4 - Response amplitude after 19 iterations, T = 440 kN
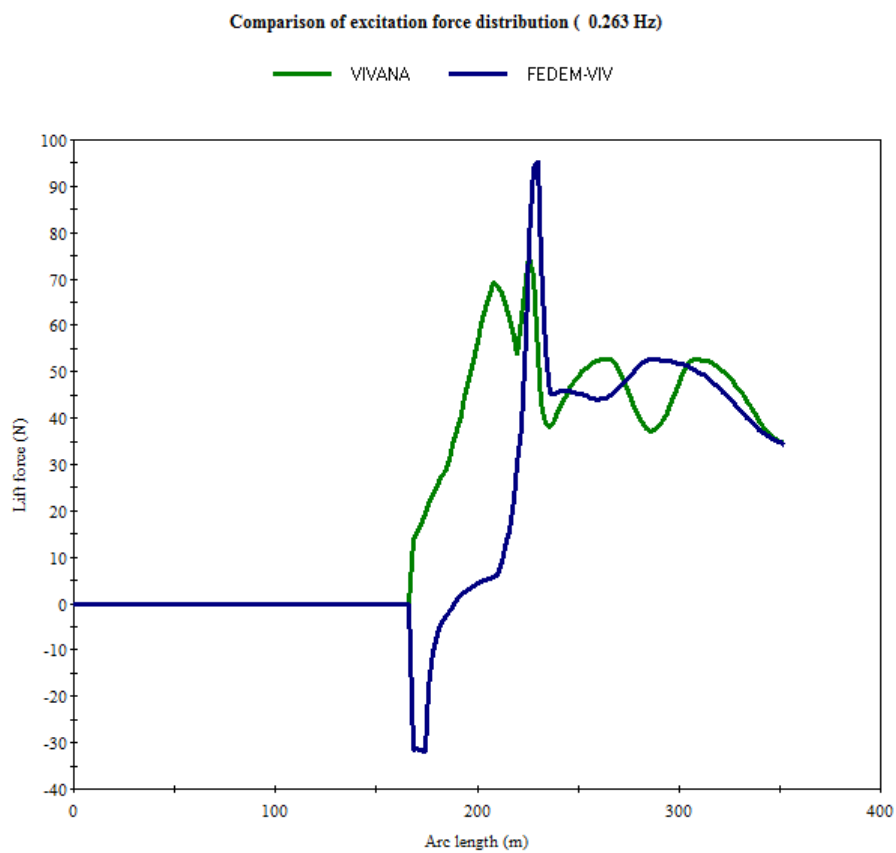
FIGURE 4.14: Comparison of excitation force distribution after 19 iterations, T = 440 kN
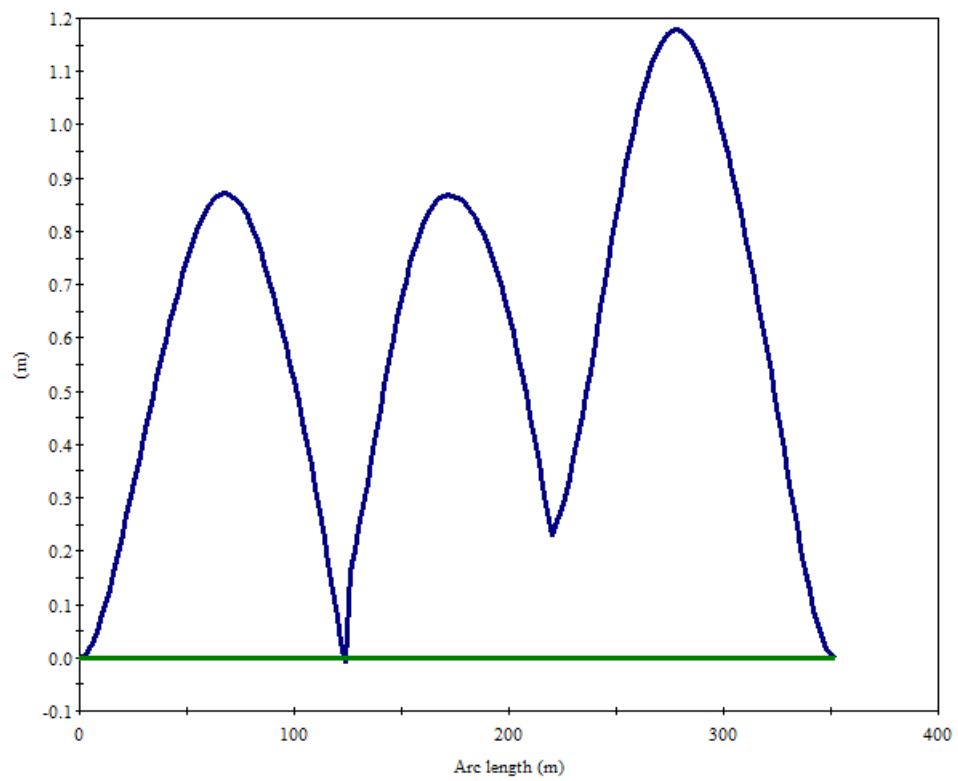
FIGURE 4.15: Case 5 - Response amplitude after 200 iterations, T = 440 kN
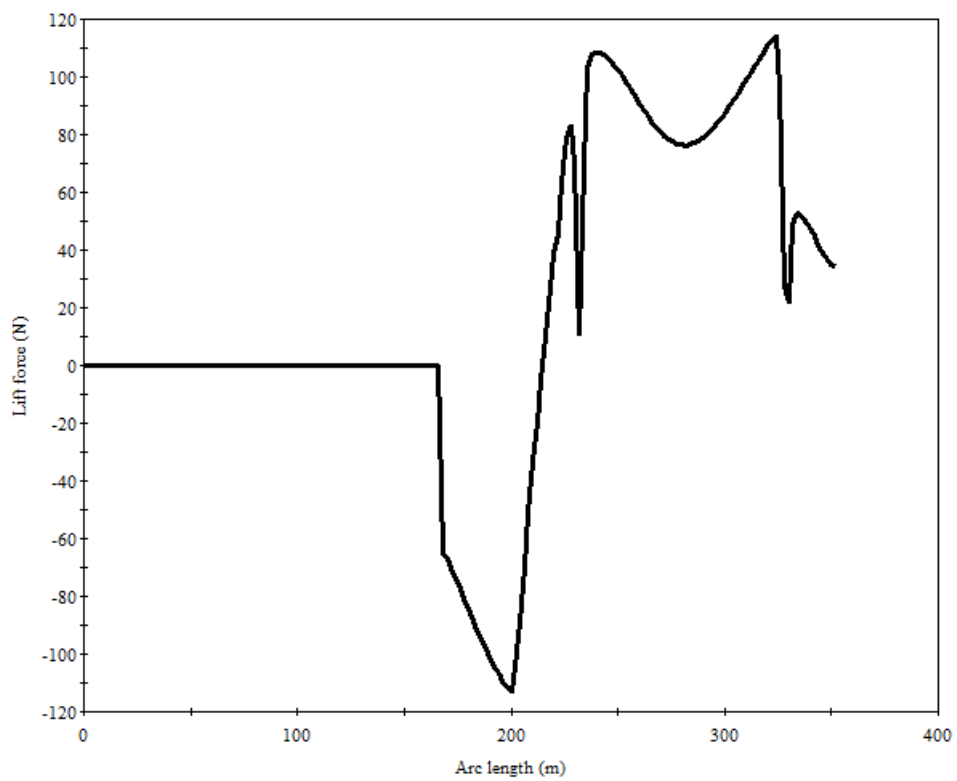
FIGURE 4.16: Case 5 - Excitation force distribution after 200 iterations, T = 440 kN

4.5 Results: T = 510 kN

The following will present the results from the T = 510 kN analysis.

4.5.1 Response frequency results

As expected, increasing the tension will also increase the natural frequency of the TTR. The dominating response frequency according to VIVANA belongs to mode number 4 as previously seen and is $f_{osc} = 0.2653$ Hz, which is a small increase from before.

| Freq. no.	Natural freq. [Hz]	Response freq. [Hz]	γ_{exc}	Length [m]
VIVANA: T = 510 kN				
1	0.0739	0.0785	0.1486	56
2	0.1548	0.1549	0.5680	38
3	0.2487	0.2277	3.2917	14
4	0.3593	0.2653	4.0490	182

TABLE 4.5: T = 510 kN, response data as computed by VIVANA

Comparing the the frequencies found by FEDEM-VIV in table 4.6 with table 4.5, the dominating frequency identified by FEDEM-VIV corresponds better with VIVANA now. This might be an effect of the increased elastic forces overshadowing potential uncertainties caused by added mass as the stiffness is increased.

Freq. no.	Natural freq. [Hz]	Response freq. [Hz]	γ_{exc}	Length [m]
FEDEM-VIV: T = 510 kN				
1	0.0739	0.0825	0.1672	50
2	0.1548	0.1548	0.5697	32
3	0.2486	0.2170	3.0443	16
4	0.3592	0.2377	3.3552	185

TABLE 4.6: T = 510 kN, response data as computed by FEDEM-VIV

However, the dominating excitation lengths agrees well within two beam element lengths, as shown in figure 4.17. Applying the same methodology of validation as before, the dominating frequency $f_{osc} = 0.2653$ Hz with an excitation length of 182 meters will be further investigated in the next section.

FEDEM-VIV vs. VIVANA excitation zones
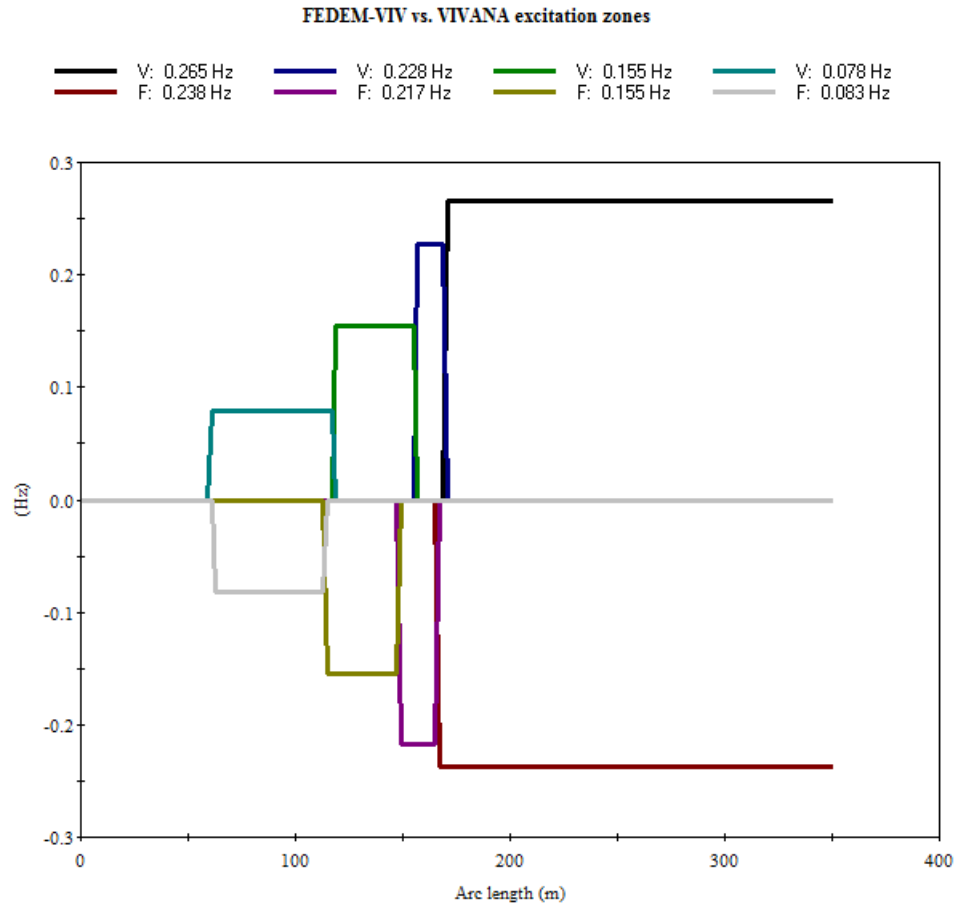
FIGURE 4.17: Comparison of excitation zones, T = 510 kN

	Response freq. [Hz]	Length [m]
VIVANA	0.2653	182
FEDEM-VIV	0.2377	185

TABLE 4.7: T = 510 kN, comparison of dominating VIV response

4.5.2 Dynamic response results

In the dynamic response analysis of the TTR with T = 510 kN, the response frequency to be investigated is $f_{osc} = 0.2654$ Hz, as computed by VIVANA. A similar testing framework based on the previous validation work is applied here, as shown in table 4.8.

Case	Iteration limit	Criteria for $C_L < 0$
6	200	fixed: $C_L = -0.05$
7	200	$C_{L,floor} = -0.1$

TABLE 4.8: T = 510 kN, FEDEM-VIV test cases

VIV response from case 6 with fixed C_L is shown together with the response from VIVANA in figure 4.18. The algorithm found the smallest accumulation of residual forces after 198 iterations. As seen, the FEDEM-VIV response is clearly overestimated with $A/D \approx 1$, in contrast to $A/D \approx 0.8$ in average in VIVANA. The corresponding excitation force distribution for case 6 in figure 4.19 shows in addition little resemblance with the prediction from VIVANA, except for a downscaled similarity between 200 and 240 meters of the TTR.
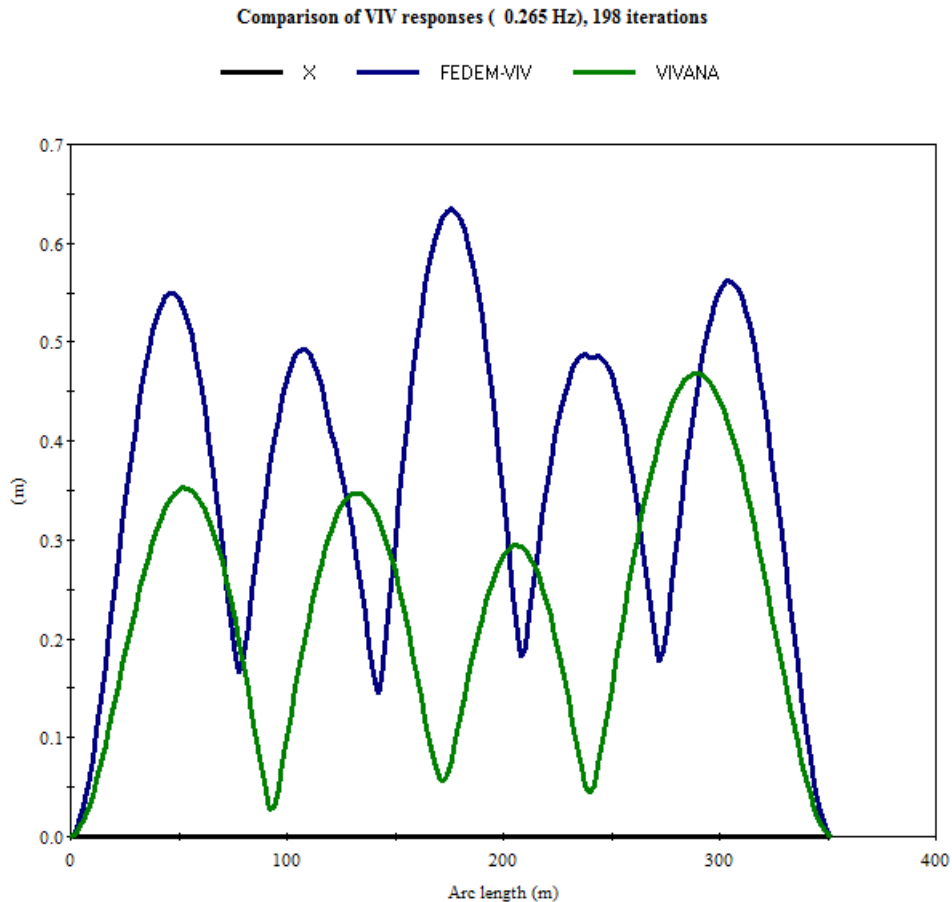

FIGURE 4.18: Case 6 - Comparison of responses for frequency 0.2653 Hz, T = 510 kN

Case 7 yields the best prediction after only 30 iterations. Comparing the VIV response with VIVANA in figure 4.20 shows different response shapes. However, it shows that the maximum amplitude is similar to the predicted value in VIVANA. With a lower limit of the lift coefficient, the excitation force distribution for case 7 in figure 4.21 shows good agreement with VIVANA, although not capturing the damping forces entirely. The force peak at around 230 meters, and the rest of the TTR to sea level, is predicted by FEDEM-VIV to be in good agreement VIVANA.
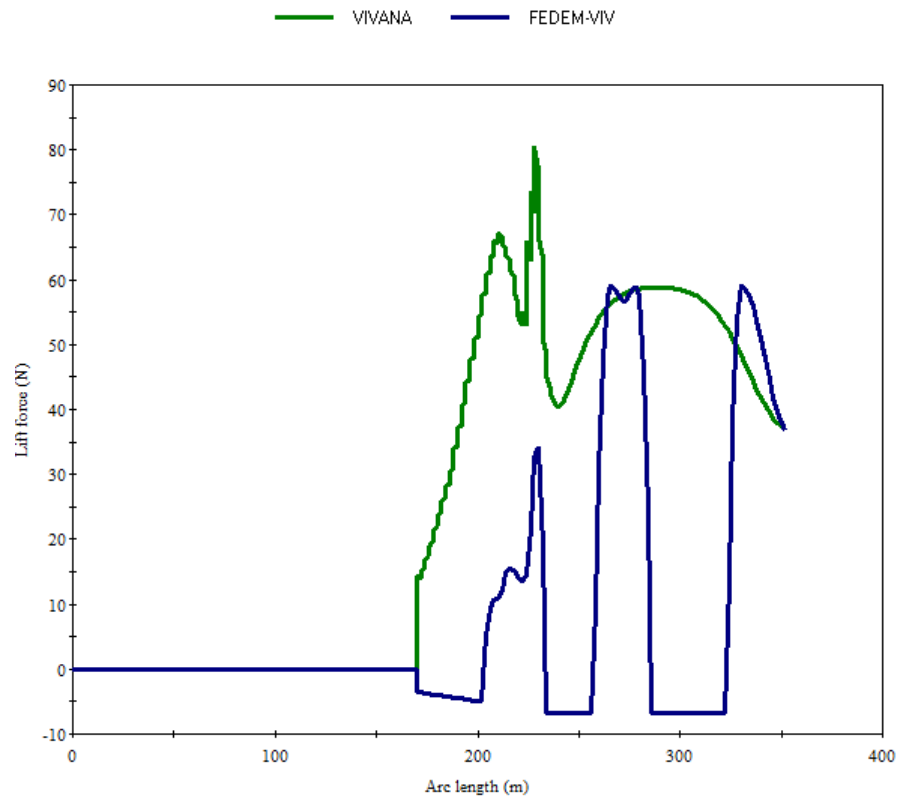
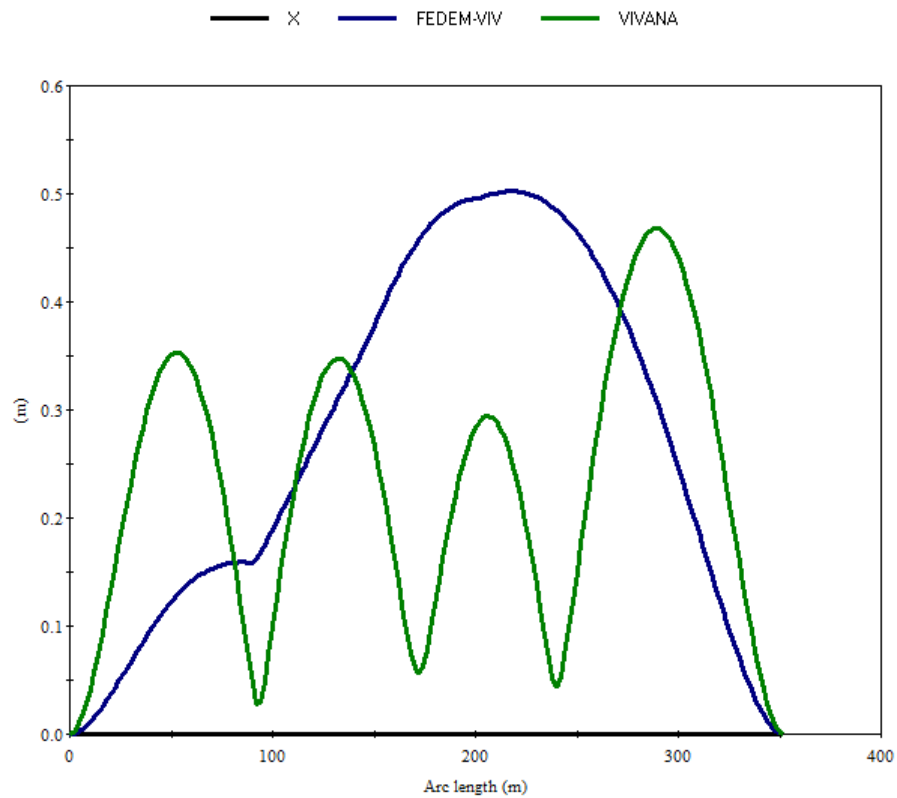FIGURE 4.19: Case 6 - Comparison of excitation force distribution after 198 iterations, T = 510 kN

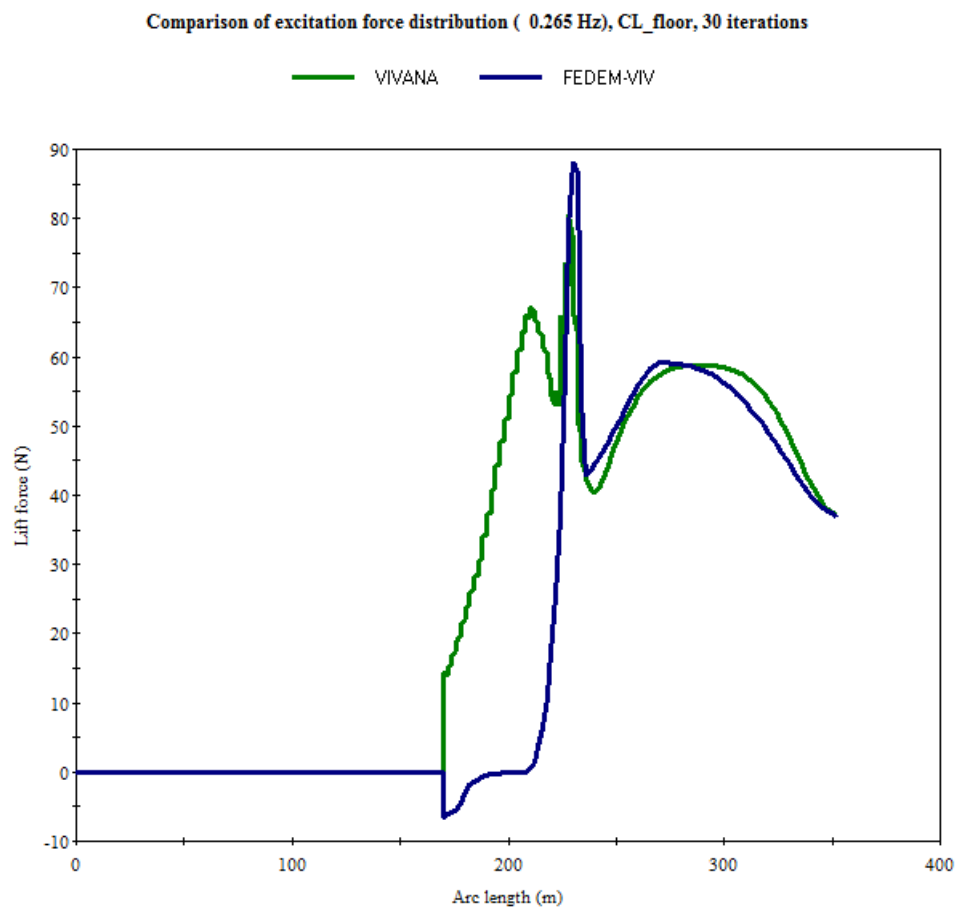FIGURE 4.20: Case 7 - Comparison of responses for frequency 0.2653 Hz, T = 510 kN

FIGURE 4.21: Case 7 - Comparison of excitation force distribution after 30 iterations,
T = 510 kN

Chapter 5

Conclusion and future perspectives

An analysis tool for prediction of VIV on marine risers has been developed in FEDEM. The methodology behind the tool is a combination of frequency and time domain models that is able to handle non-linear effects. Empirical models and its hydrodynamic coefficients as needed in a VIV analysis are adopted into FEDEM-VIV. A force prediction algorithm has been implemented in order to calculate amplitude-dependent excitation forces, allowing a time domain analysis to apply frequency domain-based models. In addition, a pragmatic approach to capture hydrodynamic damping forces is introduced to easily obtain maximum response amplitudes.

Validation studies have been carried out for a 352 meter top tensioned riser subjected to sheared current, and a great effort was made to validate FEDEM-VIV against VI-VANA. Seven test cases were developed with different number of iterations and criteria for capturing damping forces. For the cases where the lift coefficient was fixed, the predicted maximum amplitudes were within a range of 8% from VIVANA, although case 6 showed somehow overvalued amplitudes. The overall response shape is however not well captured. For the cases with a lower limit of the lift coefficient, the predicted excitation force distribution by FEDEM-VIV was in better agreement with VIVANA than for the former cases.

The validation studies show that further tuning of damping forces in FEDEM-VIV should be carried out to obtain same response shape as found in VIVANA. The lift forces should be applied as sinusoidal to capture the phase shifts. This will significantly improve the capture of the response shape envelope. More accurate response frequencies can be obtained by further investigation into how the procedure for Morison forces affects the system mass matrix in FEDEM, especially for risers with low tension.

However, with these uncertainties and simplifications in mind during development, the current approach represents a good solution for a time domain VIV predictor when all the essential hydrodynamical effects are accounted for in FEDEM-VIV. The force prediction algorithm, as its name suggests, is force-oriented. A tuning of the algorithm to predict displacement could improve the procedure. In addition, the algorithm tends to suggest higher displacements as the iteration limit increases. A different start value for the initial force or implementing a search pattern algorithm could yield more iteration consistent results. Nonetheless, a comparison of the excitation force distribution between FEDEM-VIV and VIVANA in case 7 showed good agreement, when high amplitude damping is disregarded.

Further research into applying frequency domain based models into a transient time domain simulation should be carried out to capture the response shape of a riser. Analyzing VIV in a non-linear time domain model is needed, especially since fatigue damage generally occurs in non-linear areas of a structure. The validation study has shown that FEDEM-VIV has the potential to be a feasible procedure, but more efforts, in addition to extensive validation studies, are needed for this approach to be used in practical engineering.

FEDEM-VIV differs from existing software solutions such as VIVANA and SHEAR7 by analyzing in the time domain instead of the common frequency domain approach. The presented approach introduces a more powerful and accurate analysis model. Non-linear boundary conditions and axial interactions can be accounted for in addition to currents being able to vary in both magnitude and direction with time. Risers with VIV suppression devices such as strakes can be included by importing empirical data from experiments.

Appendix A

Risk assessment

NTNU		Utarbeidet av	Nummer	Dato
HMS		HMS-avd.	HMSRV2601	22.03.2011
		Godkjent av		Erstatter
		Rektor		01.12.2006

Kartlegging av risikofylt aktivitet

Dato: 13.01.2014

Enhet: IPM

Linjeleder: Bjørn Haugen

Deltakere ved kartleggingen (m/ funksjon): George Lee, student.
(Ansv. veileder, student, evt. medveiledere, evt. andre m. kompetanse)

Kort beskrivelse av hovedaktivitet/hovedprosess: Masteroppgave George Lee: Prediction of Vortex Induced Vibrations on top tensioned marine risers.

Er oppgaven rent teoretisk? (JA/NEI): **JA** *«JA» betyr at veileder innestår for at oppgaven ikke inneholder noen aktiviteter som krever risikovurdering. Dersom «JA»: Beskriv kort aktiviteten i kartleggingskjemaet under. Risikovurdering trenger ikke å fylles ut.*

Signaturer: *Ansvarlig veileder:* Bjørn Haugen   *Student:* George Lee

ID nr.	Aktivitet/prosess	Ansvarlig	Eksisterende dokumentasjon	Eksisterende sikringstiltak	Lov, forskrift o.l.	Kommentar
1	Kontorarbeid med datamaskin	George Lee	NTNUs dokumentasjoner for HMS på arbeidsplassen	Tilrettelegging av arbeidsplassen	Arbeidsmiljøloven Arbeidsplass-forskriften	

Bibliography

[1] Robert D. Blevins. *Flow-induced vibration*. Von Nostrand Reinhold, 2nd. edition, 1990.

[2] Madan Venugopal. *Damping and Response Prediction of a Flexible Cylinder in a Current*. Phd thesis, Massachusetts Institute of Technology, MA, USA, 1996.

[3] Kyrre Vikestad, Carl M. Larsen, and J. Kim Vandiver. Norwegian deepwater program: Damping of vortex-induced vibrations. In *Offshore Technology Conference, Houston*, May 2000.

[4] Turgut Sarpkaya. *Wave Forces on Offshore Structures*. Cambridge University Presss, 2010.

[5] Robert D. Blevins. Models for vortex-induced vibration of cylinders based on measured forces. *Journal of Fluids Engineering, ASME*, 2009.

[6] Carl M. Larsen, Kyrre Vikestad, Rune Yttervik, Elizabeth Passano, and Gro Sagli Baarholm. *VIVANA - Theory Manual Version 3.4*. MARINTEK, 2005.

[7] Carl M. Larsen. *VIV - A short and incomplete introduction to fundamental concepts*. Department of Marine Technology, NTNU, 2011.

[8] *DNV-RP-C205*, 2010. Det Norske Veritas.

[9] *DNV-RP-F203*, 2009. Det Norske Veritas.

[10] SHEAR7. Shear7 technology. `http://www.shear7.com`, May 2014.

[11] Carl M. Larsen, Halvor Lie, Rune Yttervik, Elizabeth Passano, Gro Sagli Baarholm, and Jie Wu. *VIVANA - Theory Manual Version 3.7*. MARINTEK, 2009.

[12] Wikipedia. Newmark-beta method. `http://www.wikipedia.org/wiki/Newmark-beta_method`, April 2014.

[13] Carl M. Larsen Halvor Lie and J. Kim Vandiver. Vortex induced vibrations of long marine risers; model test in rotating rig. In *OMAE, Yokohama*, 1997.

[14] Carl M. Larsen, Elizabeth Passano, Gro Sagli Baarholm, and Kamran Koushan. Non-linear time domain analysis of vortex induced vibrations for free spanning pipelines. In *OMAE, Vancouver*, 2004.

[15] George Lee. *A Finite Element Software Tool for Investigation of Vortex-Induced Vibration of Risers*. Thesis project, IPM, NTNU, 2013.

[16] Geir Magnus Knardahl. *Vortex Induced Vibrations of Marine Risers*. Master's thesis, IMT, NTNU, 2012.